# Evaluating Uncertainties in the Calibration of Isotopic Reference Materials and Multi-Element Isotopic Tracers (EARTHTIME Tracer Calibration Part II)

Noah M. McLean[a,b,*], Daniel J. Condon[b], Blair Schoene[c], Samuel A. Bowring[a]

[a] *Department of Earth, Atmospheric, and Planetary Sciences, Massachusetts Institute of Technology, Cambridge, MA 02139, USA*

[b] *NERC Isotope Geosciences Laboratory, British Geologic Survey, Keyworth, Nottinghamshire NG12 5GG, UK*

[c] *Princeton University, Department of Geosciences, Guyot Hall, Princeton, NJ 08544, USA*

**Abstract**

A statistical approach to evaluating uncertainties in the calibration of multi-element isotopic tracers has been developed and applied to determining the isotopic composition of mixed U-Pb ($^{202}$Pb-$^{205}$Pb-$^{233}$U-$^{235}$U) tracers used for accurate isotope dilution U-Pb geochronology. Our experiment, part of the EARTHTIME initiative, directly links the tracer calibration to first-principles measurements of mass and purity that are all traceable to SI units, thereby quantifying the accuracy and precision of U-Pb dates in absolute time. The calibration incorporates new more accurate and precise purity measurements for a number of commonly used Pb and U reference materials, and requires inter-relating their isotopic compositions and uncertainties. Similar methods can be used for other isotope systems that utilize multiple isotopic standards for calibration purposes. We also detail the inter-calibration of three publicly available U-Pb gravimetric solutions, which can be used to bring the same first-principles traceability to in-house U-Pb tracers from other laboratories. Accounting for uncertainty correlations in the tracer isotope ratios yields a tracer calibration contribution to the relative uncertainty of a $^{206}$Pb/$^{238}$U date that is only half of the relative uncertainty in the $^{235}$U/$^{205}$Pb ratio of the tracer, which was historically used to approximate the tracer related uncertainty contribution to $^{206}$Pb/$^{238}$U dates. The tracer uncertainty contribution to $^{206}$Pb/$^{238}$U dates has in this way been reduced to <300 ppm when using the EARTHTIME and similarly calibrated tracers.

*Keywords:* tracer calibration, isotopic standards, inverse methods

## 1. Introduction

Our understanding of the rates and timing of events in Earth history depends on radioisotopic dating, or geochronology. An increasing demand for seamless integration of geochronologic data acquired with multiple radioisotopic dating methods, and with astrochronology, has motivated continued improvements in measurement precision, ongoing assessment of the accuracy of parent

*Principal Corresponding Author
email: noahm@bgs.ac.uk

radionuclide decay constants, and characterization of the compositions of reference materials used for calibrations and assessment of reproducibility. U-Pb dates are ultimately derived from experiments that utilize isotope dilution principles combined with isotope ratio mass spectrometry (Stracke et al., 2014, and references therein), an approach that permits the translation of isotope ratios measured on a mass spectrometer to relative elemental abundances with very high precision. In practical terms this is achieved through admixing a homogeneous isotopic tracer with a dissolved sample, so that the accuracy of U-Pb dates are relative to and therefore ultimately traceable back to a tracer solution. Other isotopic systems that utilize multi-element tracers include Rb-Sr (e.g., Nebel et al., 2011; Rotenberg et al., 2012), Sm-Nd (e.g., Wasserburg et al., 1981), and Lu-Hf (e.g., Vervoort et al., 2004).

This paper outlines the statistical methodology applied to determining the composition and associated uncertainties of a mixed ($^{202}$Pb-$^{205}$Pb-$^{233}$U-$^{235}$U) U-Pb tracer solution. The rare artificial isotope $^{202}$Pb is included in a limited quantity of this tracer, called 'ET2535', and omitted from the rest, separately denoted 'ET535'. The methods described here can be applied to high-precision, high-accuracy calibration of other tracers, and the results can be used to compare and combine chronological information from multiple chronometers. The U-Pb tracer solution used here was created, calibrated and distributed to labs dedicated to high-precision U-Pb geochronology under the auspices of the EARTHTIME initiative. A companion paper to this one (Condon et al., in review) describes the metrologic traceability and mass spectrometry used to calibrate the tracer solution, detailing linked experiments that are underpinned by a number of primary determinations. Here we focus on building statistical models to determine maximum likelihood estimates of the isotopic composition of mixed-element tracers, using the EARTHTIME U-Pb tracer as an example.

The statistical models described here also quantify uncertainty contributions to radioisotopic dates. For the U-Pb tracer calibration, the isotopic composition of U and Pb isotopic standards that are utilized in multiple places in the calculations provide the largest contributions and the largest opportunity for improvement. Many calculated values (for instance, the U/Pb ratio and U and Pb ICs of the tracer) share this common uncertainty, so that quantifying the statistical correlation between the different experiments has become paramount in accurately estimating the uncertainty of U/Pb dates. These systematic uncertainties and others outlined in this paper, when considered with decay constant uncertainties and corrections for intermediate daughter excess/deficiencies, provide the present limit on the absolute uncertainties achievable by U-Pb geochronology. With fully traceable inputs and resulting uncertainties, this tracer calibration also provides a foundation for accurate comparison of U-Pb geochronology to other radioisotopic or non-radioisotopic dating methods similarly based on first-principles methods.

### *1.1. Isotope dilution mass spectrometry*

Isotope dilution (ID) isotope ratio mass spectrometry continues to be the most precise and accurate approach for measuring multi-element isotope ratios, such as the parent/daughter ratios used for geochronology, (e.g., $^{238}$U to $^{206}$Pb, $^{147}$Sm to $^{143}$Nd). Isotope dilution entails adding a tracer solution with one or more synthetic or artificially enriched isotopes to a sample. The concentration of a sample isotope can be estimated using the known amount of the tracer isotope and the measured sample/tracer isotope ratio. This process can be repeated for other targeted elements in the sample and tracer, and the ratio of two different elements in the sample (e.g., parent/daughter) can then be calculated. Uncertainties in the concentrations of parent and daughter elements in the tracer largely cancel, meaning the uncertainty in the desired isotope ratio or date depends on the accuracy

and precision of the parent/daughter element ratio in the tracer. Estimation of this ratio, or tracer calibration, is carried out by mixing the tracer with gravimetric reference solutions, which are usually created by dissolving large quantities (to minimize weighing errors) of isotopic or elemental reference materials that have well-determined purity and isotopic composition (Tilton et al., 1955; Wetherill, 1956; Wasserburg et al., 1981). Although the reference materials (e.g., NBS 981 for Pb, CRM 112a for U) are widely used and easily obtained, their isotopic composition and purity have uncertainties that must be quantified for a complete assessment of a tracer calibration's accuracy.

Another concern for generating accurate and precise data is correcting for intra-element isotopic fractionation that occurs during mass spectrometric analysis. To correct for short timescale fluctuations requires using a double spike, composed of two artificially enriched isotopes of the same element that is being analyzed. There are two commonly used double spike formulations. In the first, the spike isotopes are also present in the sample, but with different relative abundances (Galer, 1999; Rudge et al., 2009), for instance a $^{204}$Pb-$^{207}$Pb tracer. These double spikes require analyzing both a spiked and an unspiked aliquot of the same sample, limiting their utility for very small samples. A second type of double spike is composed of two synthetically produced isotopes that do not naturally occur in the sample. Examples include $^{202}$Pb-$^{205}$Pb tracers (Amelin and Davis (2006) and this work), and the $^{233}$U-$^{236}$U tracer (Verbruggen et al., 2008) used to inter-calibrate U reference materials below. A third type of hybrid double-spike is enriched in a synthetic isotope and a naturally occurring isotope, for instance the $^{233}$U-$^{235}$U tracer described here, which can be used to monitor instrumental isotopic fractionation when the isotopic composition of the analyte is well constrained (e.g., Krogh, 1964; Hofmann, 1971).

It is common that data generated in different laboratories are determined relative to tracers whose calibrations are not relatable, in that they may not be calibrated against the same reference materials or using the same methodology. This makes it necessary to account for tracer calibration uncertainty when comparing dates determined in different laboratories using different tracers. Though published geochronologic data often include an estimate of the uncertainty in the tracer calibration, this uncertainty is often comparable to or exceeds a date's analytical uncertainty. The tracer calibration uncertainty therefore limits the resolution of timelines constructed using data from multiple labs. For this reason, we have mixed and calibrated a ($^{202}$Pb-$^{205}$Pb-$^{233}$U-$^{235}$U) U-Pb tracer that is being utilized in a number of laboratories dedicated to high-precision isotope dilution U-Pb geochronology by thermal ionization mass spectrometry (TIMS). We also provide new traceable and inter-relatable isotopic compositions and purities for isotopic reference materials and gravimetric solutions derived from them that together can be used to calibrate other U-Pb tracers, such that their accuracy is relatable to the EARTHTIME tracer calibration. Widespread distribution and use of these U-Pb tracers removes interlaboratory bias related to tracer calibration and provides the opportunity to engage in a well-documented, transparent tracer calibration experiment that is traceable to SI units. We have attempted to identify all sources of random and systematic uncertainties that should be considered in any multi-element tracer calibration, and provide an estimate for the total tracer calibration uncertainty to be included in comparisons of dates between different dating methods.

### *1.2. Application of Inverse Methods*

Accurately and precisely relating the isotopic composition of a tracer to first principles measurements benefits from a large quantity of data: over $10^5$ measured isotope ratios are used to calibrate the EARTHTIME U-Pb tracer. Each measured isotope ratio contains information about the mixture of components being analyzed, which include small but unavoidable Pb and U contamination

known as laboratory blank, along with the tracer, an isotopic/elemental reference solution, or both. Unraveling the isotopic compositions (ICs) and relative proportions of each component is made more difficult by isotopic fractionation, or the preferential evaporation, ionization and/or detection of lighter isotopes over heavier ones, which changes in magnitude during the course of a typical TIMS analysis. A measured ratio may therefore be expressed as the amount ratio of its summed components, modified by a correction factor for isotopic fractionation. The system of equations that relates each measured ratio to the relative abundances and isotopic compositions of its components is known as the measurement model, which is derived and described in Appendix B.

To determine the relative abundances of the tracer isotopes, the inverse methods of Tarantola (2005) are applied to a series of linked experiments that represent the complete tracer calibration experiment. Each of these experiments is solved as a separate inverse problem, and a subset of the model (free) parameters in the first experiments is used to constrain solutions of the following experiments. For example, the tracer $^{233}U/^{235}U$ is a free model parameter in the U IC experiment in Section 4, the results of which are used as well-constrained 'systematic' uncertainties in Section 6. Combined, the following experiments represent the complete tracer calibration algorithm, illustrated in Figure 1:

Section 2) Inter-calibrate Pb and U ICs of all isotopic reference materials used for tracer calibration such that their covariance is determined;
Section 3) Determine the Pb IC of the tracer and the blanks, and their covariance;
Section 4) Use critical mixtures of the tracer and multiple U isotopic reference materials to estimate the U IC of the tracer and its covariance when the natural U IC of a sample is related;
Section 5) Determine the U/Pb ratios of the gravimetric solutions using measurements of mass, purity, and the ICs of their constituent Pb and U reference materials;
Section 6) Combine results from all previous calculations to estimate the $^{235}U/^{205}Pb$ and $^{202}Pb/^{205}Pb$ ratio of the tracer using mixtures of the tracer with three gravimetric solutions.

## 2. Inter-calibration of Pb and U Isotope Reference Materials

In order to determine the U/Pb ratio of the EARTHTIME tracers, each was mixed with three gravimetric solutions that have U and Pb concentrations determined by weighing and a gravimetrically traceable isotopic composition. The solutions are composed of three different Pb reference materials, NBS 981, NBS 982 and 'Puratronic Pb', along with two different U reference materials, CRM 112a and CRM 115. An additional U reference material, U500, was used during evaluation of the uranium IC of the tracers using critical mixtures; see (Condon et al., in review) for a more complete description of each of these reference materials. The tracer uranium IC is then used in the fractionation correction equations for the gravimetric-tracer mixture data reduction (Fig. 1).

Because all six isotopic reference materials are used to determine the tracer U/Pb ratio, their uncertainties all contribute to the final uncertainty budget of the tracer IC, and any correlation between the uncertainties in their ICs must be considered when averaging the results from the three gravimetric solutions. Uncertainty correlations result from relating the ICs of the reference materials to SI units, accomplished for both U and Pb by measuring the isotope ratios of the reference materials against a single independent gravimetrically calibrated isotope ratio, a process known as inter-calibration.

### 2.1. Pb Isotope Reference Material Inter-calibration

Unlike the well-characterized IRMM-3636(a) U isotopic reference solution (see below), there is no gravimetric mixture of synthetically produced isotopes against which Pb isotopic reference materials can be measured. However, the NBS 981, 982, and 983 reference materials have been calibrated by sample-standard bracketing with mixtures of high-purity $^{208}$Pb and $^{206}$Pb that were gravimetrically mixed to mimic the $^{208}$Pb/$^{206}$Pb of the reference materials (Catanzaro et al., 1968). As such, these determinations may be considered traceable to SI units.

Modern mass spectrometric measurements are significantly more precise than those of Catanzaro et al., and modern laboratory protocols have significantly lower contamination levels, or laboratory blanks, to bias the measurements. Because the original high-purity $^{208}$Pb and $^{206}$Pb are no longer available, the absolute uncertainties of Pb reference materials cannot be improved with new measurements, but the relative uncertainties between them may be significantly refined. For this purpose, the ICs of Pb isotopic standards have been revisited multiple times since their original certification (e.g., Todt et al., 1996; Doucelance and Manhès, 2001; Baker et al., 2004), all of which base their results on an assumed value of $^{208}$Pb/$^{206}$Pb of NBS 981 or 982 from Catanzaro et al. (1968). In these studies and in ours, fractionation lines for the standard measurements lie within $2\sigma$ uncertainties of the certified ICs of NBS 981 and 982.

The isotopic composition of NBS 981 is closer to that of modern terrestrial Pb, and therefore laboratory blank Pb, so that blank corrections for even small samples of NBS 981 result in negligible changes in blank-corrected IC. We therefore choose to base our calibration on the gravimetrically traceable Catanzaro et al. (1968) isotopic composition of NBS 981, and assume the value and total uncertainty of its $^{208}$Pb/$^{206}$Pb of $2.1681 \pm 0.0008$ ($2\sigma$). The reported $2\sigma$ uncertainty is derived from a 95% confidence interval calculated with linear, rather than quadratic addition, and is therefore likely to be a conservative estimate of the true precision of the original measurement. The Pb isotopic composition of NBS 981, NBS 982 and Puratronic Pb reported in Tables 3 and 4 are calculated relative to the $^{208}$Pb/$^{206}$Pb of NBS 981, and do not represent absolute measurements of their Pb isotopic composition.

To inter-calibrate the Pb isotopic reference materials used to create the gravimetric solutions, we used the raw data for measurements of NBS 981, NBS 982, and Puratronic Pb reported in Amelin and Davis (2006), along with several analyses of the same reference materials from the same laboratory using the same methods (Fig. 2), with all data compiled and reported in (Condon et al., in review). Given one of the goals of this intercalibration is to account for mass independent fractionation, which requires measuring large aliquots of solution, the Amelin and Davis (2006) data are used instead of separate measurements utilizing ET2535 in order to avoid a large expenditure of relatively scarce $^{202}$Pb. Smaller loads of the gravimetric solutions with ET(2)535 were thus used to calibrate the U/Pb ratio of the tracer using accurate Pb reference material ICs derived from published data.

### 2.2. U Isotope Reference Material Inter-calibration

To relate the isotopic compositions of the U reference materials to one another, we measured each against IRMM 3636(a), which was created by weighing highly pure $^{233}$U and $^{236}$U and mixing them in a 1:1 ratio (Verbruggen et al., 2008). Because the artificial isotopes that comprise IRMM 3636(a) have been weighed against an in-house kilogram reference, its precisely determined $^{233}$U/$^{236}$U is traceable to the SI system, and ICs that have been measured against it are relatable to the SI

through their measurement uncertainties and to one another by tracing each measurement back to SI units.

In this way, the $^{238}U/^{235}U$ ratios and uncertainties for the reference materials SRM U500 and CRM 112a can be related using the supplementary data from Condon et al. (2010), which reports the derivative, or linear dependence, of each measured IC with respect to IRMM 3636(a). New data for the U reference material CRM115 is provided in the supplementary data of this publication, and is reduced using the same algorithms as Condon et al. (2010).

No correlations between the isotope ratio uncertainties are reported on the IRMM 3636 certificate of analysis, so they are assumed to be uncorrelated. The uncertainty in the IC of IRMM 3636(a) is treated here as a systematic uncertainty among the reference material analyses. CRM 115 and CRM U500 are both synthetic reference materials and thus contain $^{236}U$. The $^{233}U/^{236}U$ values for each were measured for un-spiked aliquots, and then this source of $^{236}U$ was subtracted before using the $^{233}U/^{236}U$ of IRMM 3636(a) to determine the magnitude of isotopic fractionation.

### *2.2.1. Algorithm*

The six equations in the system (B.5) describe the anticipated outcome of measuring a mixture of Pb isotopic reference material with laboratory blank and a $^{202}Pb$-$^{205}Pb$ tracer that is undergoing both mass-dependent and mass-independent fractionation in the presence of a $BaPO_2$ isobaric interference. Several of the variables on the right hand side of equations (B.5), along with their uncertainties, can be constrained *a priori*. For instance, the IC of the non-enriched tracer components, along with an average loading blank mass and their uncertainties, can be estimated with the algorithm in Section 3. The approximate $BaPO_2$ IC is calculated from the approximate natural abundances of its component elements (Böhlke et al., 2005), which are assumed to fractionate by 0.1% per u during analysis, and are assigned a 2% prior uncertainty. The relative uncertainties in the isotopic masses of the Pb isotopes are at the ppb level (Audi et al., 2003), and their uncertainties are not propagated here. Finally, a single gravimetric Pb reference material isotope ratio is required to calibrate $r25t$, the $^{202}Pb/^{205}Pb$ ratio of the tracer, which can then be used to fractionation-correct the remaining two gravimetric reference material Pb ICs.

Parameters treated as unknowns include the $^{202}Pb/^{205}Pb$ ratio of the tracer, and the Pb ICs of the gravimetric solutions, excluding the single assumed ratio. Although the gravimetric solution and tracer masses were weighed prior to mixing, a far more precise estimate of their relative abundance, represented by the ratio of $^{206}Pb$ in the gravimetric solution to the $^{202}Pb$ in the tracer, can be calculated using mass spectrometer measurements, and so this parameter is treated as an unknown. The three parameters that describe an instantaneous state of mass-independent fractionation, $\gamma_{205}$, $\gamma_{207}$, and $\beta$ (see Appendix B.1), are also treated as unknowns. Thus, multiple measurements of several Pb reference materials mixed with the same $^{202}Pb$-$^{205}Pb$ tracer define a system of equations, and the model in (B.5) relates the measured values to the physical parameters of interest.

### *2.2.2. Results*

The highest-precision data reported in Amelin and Davis (2006) were used for each reference material: ten NBS 981, nine NBS 982, and four Puratronic Pb analyses. Each is reported as several block means and standard errors, with isotope ratios relative to $^{206}Pb$, as in equations (B.5), and the measured ratio uncertainties are assumed to be uncorrelated. To avoid uncorrected isobaric interferences, which usually occur at the beginning or end of an analysis and significantly displace the block mean from the trend defined by the majority of the data, all block data for each analysis were

plotted in $^{202}Pb/^{206}Pb$ - $^{204}Pb/^{206}Pb$ - $^{207}Pb/^{206}Pb$ - $^{208}Pb/^{206}Pb$ coordinates, and any outliers were rejected from further consideration. Plots of the included and excluded block data are shown in the electronic supplement.

After outlier rejection, there are 160 blocks each of NBS 981 and NBS 982, and 36 blocks of Puratronic Pb, each consisting of six measured ratios and uncertainties, for a total of 2136 isotope ratio measurements. This is the length of the vector $\mathbf{d}$ in the model described in Appendix A. These data can be used to constrain the 824 model parameters in the vector $\mathbf{m}$ needed to describe them: three Pb ratios for each gravimetric Pb reference material, five Pb ratios for the IC of the tracer used, three $BaPO_2$ isotope ratios, three Pb blank ratios, unique values to quantify the ratios of gravimetric solution and laboratory blank to the isotopic tracer and the mass-independent fractionation of $^{205}Pb$ and $^{207}Pb$ for each of the 23 analyses and a unique magnitude of mass-dependent fractionation ($\beta$) and level of $BaPO_2$ interference for each of the 356 included blocks. This defines an over-determined system that can be solved by conventional non-linear least squares techniques. We employed an iterative method known as preconditioned gradient descent (Tarantola, 2005) to minimize the misfit function in equation (A.1), which was executed in MATLAB. Initial values for the model parameters were calculated using a linearized form of equations (B.5), and the derivatives required were calculated analytically for each iteration. The MATLAB code is provided in the electronic supplement.

In this model, the assumed $^{208}Pb/^{206}Pb$ ratio of NBS 981, as well as the blank, and $BaPO_2$ ICs and the ratios of $^{204}Pb$, $^{206}Pb$, $^{207}Pb$, and $^{208}Pb$ to $^{205}Pb$ in the tracer act as systematic uncertainties, whose values and uncertainties are known *a priori*. The measurement uncertainties are calculated by approximating the nonlinear function $G(\hat{\mathbf{m}})$ with its Jacobian matrix evaluated at the solution, denoted $G$. The matrix $G$ has 2136 rows and 824 columns that contain the derivative of each of the 2136 predicted values with respect to the 824 model parameters. The measured uncertainties are estimated using equation (A.2).

In order to estimate the component of uncertainty arising from systematic effects, the system was solved for 5000 Monte Carlo realizations of these systematic parameters, created with a pseudorandom number generator to have a multivariate normal distribution with a covariance structure corresponding to their assumed uncertainties. Thus the system with 2136 measurements and 824 model parameters was solved 5000 times, once with each Monte Carlo realization of the systematic parameters, which were given extremely small prior uncertainties to ensure that the least-squares solution converged to their input values. The uncertainty in the unknown model parameters calculated from the inverse model solution using the best estimates of the systematic parameters, for instance with the $^{208}Pb/^{206}Pb$ of 981 equal to 2.1681 with infinitesimal uncertainties, defines their measured uncertainties.

For the model parameters treated as unknowns, the distribution of the resulting 5000 solutions defines the probability distribution of the model parameters resulting from the input systematic uncertainties. The data plotted in Fig. 4 for the $^{208}Pb/^{206}Pb$ of NBS 982 confirms that the modeled output data is well-approximated by a Gaussian distribution, and the same holds for the other isotope ratios of the gravimetric Pb reference materials. The results of all Monte Carlo trials are included in the electronic supplement.

The systematic uncertainties in the model parameters may therefore be estimated by evaluating the mean and covariance matrix of the 5000 estimates of $\hat{\mathbf{m}}$, denoted $\tilde{C}_{\mathrm{M}}^{sys}$. The total systematic and measurement uncertainties, estimated with equations (A.2) and (A.3) are given in Table 3, and the correlation coefficients between them, derived from $\tilde{C}_{\mathrm{M}}^{tot}$, are provided in Table 4.

## 3. Determining the Pb IC of the Tracer and Blank

It is not possible to accurately measure the isotopic composition of the tracer and the loading blank independently. For the TIMS method, all measurements involve a "loading blank" derived from mixing tracer with a silica gel activator, which has a finite Pb blank, with the possibility of introducing additional blank by pipetting the combined solution onto the filament and later exposing the loaded filament to atmosphere. Mass spectrometry by ICP-MS is similarly affected by Pb blank contributions from reagents and carrier gases, as well as interferences from other elements such as Hg and Tl. The IC of the Pb blank is also problematic to analyze alone because small (e.g. <0.3 pg) blanks produce weak ion beams (e.g. less than ca. 20 cps $^{204}$Pb and 800 cps $^{208}$Pb) that limit measurement precision and accuracy. In addition to the average IC of the Pb blank, its variability from load to load is an important uncertainty contribution to both the tracer calibration exercise and analyses of geologic materials (McLean et al., 2011). The practice of combining several Pb blanks into a single analysis averages out and therefore underestimates this blank IC variability.

However, since the loading blank and tracer are measured together, a linear regression algorithm can be used to estimate each. Loading and analyzing several different masses of tracer using approximately the same amount of silica gel establishes a two-component mixing line between the blank IC and the tracer IC. When plotted in $^{204}$Pb/$^{205}$Pb - $^{206}$Pb/$^{205}$Pb - $^{207}$Pb/$^{205}$Pb - $^{208}$Pb/$^{205}$Pb coordinates, the tracer IC occupies a unique point on this line and the blank IC is defined by its slope. The correct tracer and blank IC together are important for accurately interpreting U-Pb data, especially data with lower Pb*/Pbc ratios (e.g. Rioux et al., 2012).

### *3.1. Determining the mixing line parameters*

The algorithm presented in McLean (2014) calculates the best fit line through data with correlated uncertainties in two or more dimensions, and is well-suited to a four-dimensional mixing model. In this model, a measured mixture of tracer and blank falls on a mixing line that follows the equation

$$\begin{bmatrix} \left(\frac{^{204}\mathrm{Pb}}{^{205}\mathrm{Pb}}\right)_{mix} \\ \left(\frac{^{206}\mathrm{Pb}}{^{205}\mathrm{Pb}}\right)_{mix} \\ \left(\frac{^{207}\mathrm{Pb}}{^{205}\mathrm{Pb}}\right)_{mix} \\ \left(\frac{^{208}\mathrm{Pb}}{^{205}\mathrm{Pb}}\right)_{mix} \end{bmatrix} = \begin{bmatrix} \left(\frac{^{204}\mathrm{Pb}}{^{205}\mathrm{Pb}}\right)_{tr} \\ \left(\frac{^{206}\mathrm{Pb}}{^{205}\mathrm{Pb}}\right)_{tr} \\ \left(\frac{^{207}\mathrm{Pb}}{^{205}\mathrm{Pb}}\right)_{tr} \\ \left(\frac{^{208}\mathrm{Pb}}{^{205}\mathrm{Pb}}\right)_{tr} \end{bmatrix} + \begin{bmatrix} 1 \\ \left(\frac{^{206}\mathrm{Pb}}{^{204}\mathrm{Pb}}\right)_{bl} \\ \left(\frac{^{207}\mathrm{Pb}}{^{204}\mathrm{Pb}}\right)_{bl} \\ \left(\frac{^{208}\mathrm{Pb}}{^{204}\mathrm{Pb}}\right)_{bl} \end{bmatrix} \cdot \tau_{Pb} \quad (1)$$

where $mix$, $tr$, and $bl$, correspond to the mixture, tracer, and blank components, respectively, and $\tau_{Pb}$ is the ratio of the moles of $^{204}$Pb contributed from the blank to the moles of $^{205}$Pb from the tracer, which varies from analysis to analysis. This is a parametric equation for a line of the form $\mathbf{p}_i = \mathbf{a} + \mathbf{v}\,\tau_i$, where the vector $\mathbf{a}$ is a point on the line corresponding to the tracer IC, as above, and the vector $\mathbf{v}$ describes the direction in which the tracer composition is perturbed by the addition of loading blank. Each measured mixture IC vector $\mathbf{p}_i$ is assigned an uncertainty in the form of a covariance matrix that incorporates measurement and fractionation-correction effects.

Using the measurement uncertainties to weight the line fit assumes that the deviation of each measurement from the best fit line is due only to the assigned measurement uncertainty and that the blank has a single, constant IC. In a dataset of measured tracer-blank mixes, the IC of the blank is expected to vary because it reflects a mixture of Pb from several sources. For this experiment, the Pb blank combines Pb in the silica gel emitter, Pb obtained from the phosphoric and hydrochloric acid used to dry down the tracer, Pb on the surface of the beaker used for drying and the inner surface of the pipette used for loading, as well as any particulate matter from the inside of the laminar flow bench on which the sample was dried down. Although these often sum to <0.3 pg of total Pb blank (e.g., Rioux et al., 2012), the ICs of the sources are likely variable, as are their relative contributions, resulting in a Pb blank with variable IC. This would create scatter from the mixing line between the tracer IC (assumed constant) and the mean blank IC beyond that expected from measurement uncertainties alone.

A dataset comprising 22 measurements of loading blank-tracer mixtures exhibits overdispersion with a mean square weighted deviation of 39. To correctly account for the blank IC variability as an additional source of scatter, an uncertainty term must be added to each point that is proportional in magnitude to the amount of blank present. Thus, a point on the mixing line close to the IC of the tracer would be perturbed minimally, while a point farther away would be more sensitive to variation in the blank IC. The overdispersion will affect the measured $^{206}Pb/^{205}Pb$, $^{207}Pb/^{205}Pb$, and $^{208}Pb/^{205}Pb$ relative to the measured $^{204}Pb/^{205}Pb$, and these effects will be correlated: the blank IC is expected to be variable, but to generally trend between more and less radiogenic Pb ICs.

To calculate the variability in the blank IC from the measured data, a trial tracer IC was first determined by fitting a line to the measurement data using the measurement uncertainties only. This trial tracer IC was subtracted from each measured mixture, and the measurement and fractionation correction uncertainties were propagated to calculate $^{206}Pb/^{204}Pb$, $^{207}Pb/^{204}Pb$, and $^{208}Pb/^{204}Pb$ ratios and covariance matrices for each measurement. The scatter in the resulting estimated blank ICs cannot be explained by measurement uncertainties alone (Fig. 6).

Neglecting the measurement uncertainties and calculating the $2\sigma$ covariance ellipse for the discrete ratio data will overestimate the true variability of the tracer, since it does not consider the extra scatter caused by measurement uncertainties. Alternatively, the scatter in the Pb blank ICs may result from the sum of two different multivariate normal distributions: the individual measurement uncertainty unique to each data point and a blank IC variability that affects all data points. The maximum likelihood estimate of the covariance matrix for this 'extra scatter' (Vermeesch, 2010) is shown in green in Figure 6. It is smaller than the discrete data covariance ellipse, and the lower correlation coefficients demonstrate that part of the high correlation of the measured data is due to the high correlation of the measured uncertainties.

In order to account for the excess scatter from the variable Pb blank IC, the overdispersion covariance matrix must be added to the uncertainty in each measured data point, multiplied by a factor proportional to the distance from the point to the tracer IC. This factor increases linearly with distance along the line from the tracer IC, where it is zero. A new line was fit to the data with these increased uncertainties, a tracer IC chosen, and the overdispersion calculated; iterating these steps quickly converges on the tracer IC, and the uncertainties in the line parameters now reflect all sources of scatter.

### *3.2. Results*

Estimates for the tracer and blank ICs are given in Table 5. Although the tracer IC is constrained to be on the mixing line (Fig. 5), there are only two physical constraints on its location. First, the isotope ratios that comprise it must not be negative. Second, the proposed IC must have less of the common Pb components than the analysis with the highest ratio of tracer to blank. These two endpoints define a line segment along which the tracer IC must lie, and it will be shown that the location chosen does not influence the value or uncertainty budget of an analysis that has been corrected for both tracer and blank. The tracer IC in Table 5 has been arbitrarily chosen to have a composition halfway between the two possible endpoints of this line segment, and its $2\sigma$ uncertainty is set to the half-length of the segment (Fig. 5).

The line fit algorithm of McLean (2014) outputs uncertainties for a point on the line (the tracer IC) and the slope of the line (the blank IC), given in Table 5. The uncertainties in the tracer IC ratios are strongly correlated, as are the blank IC ratios, with correlation coefficients given in Table 6. The magnitude of the uncertainties in the tracer IC and their correlation define an uncertainty envelope around the tracer IC that is parallel to the tracer-blank mixing line.

### *3.3. Application to TIMS Pb measurements*

Although the blank and tracer ICs may be expressed separately, both components must be subtracted from routine analyses. Therefore it is their sum, which is constrained to fall along the mixing line, that is of interest. There are two approaches to blank subtraction currently employed for ID-TIMS analyses, used when analyses contain $^{204}$Pb masses consistent with total procedural blank measurements, for example chemically abraded zircon, or contain initial common Pb, for example titanite, apatite, or perovskite (Corfu and Dahlgren, 2008; McLean et al., 2011; Schmitz and Schoene, 2007).

In the first approach, all $^{205}$Pb comes from the tracer and all $^{204}$Pb from the tracer and the blank. The measured and fractionation-corrected $^{204}$Pb/$^{205}$Pb defines a unique location on the tracer-blank mixing line. The corresponding $^{206}$Pb/$^{205}$Pb, $^{207}$Pb/$^{205}$Pb and $^{208}$Pb/$^{205}$Pb on the line are those of the tracer-blank mixture, which are subtracted from the measured, fractionation-corrected ratio (McLean et al., 2011). Both the uncertainties in the mixing line parameters and the measured $^{204}$Pb/$^{205}$Pb are propagated into the tracer- and blank-corrected ratios.

In the second approach to common Pb correction, the mass of the Pb blank is assumed based upon some prior knowledge, and the estimated masses of tracer and blank are subtracted together from the fractionation-corrected measured IC of the sample. The rest of the common Pb (including $^{204}$Pb) is considered part of the sample, so the measured $^{204}$Pb/$^{205}$Pb is no longer restricted to tracer and blank components. To determine the moles of a given isotope in the sample, for instance $^{206}$Pb, first the moles of total procedural blank is determined (equation 15 of McLean et al., 2011),

$$moles\left(^{206}\mathrm{Pb}\right)_{tpb} = moles(^{205}\mathrm{Pb})_{tr} \cdot \left[ \left(\frac{^{206}\mathrm{Pb}}{^{205}\mathrm{Pb}}\right)_{fc} - \left(\frac{^{206}\mathrm{Pb}}{^{205}\mathrm{Pb}}\right)_{tr} \right] \tag{2}$$

and the total procedural blank is subtracted from a subsequent analysis

$$moles\left(^{206}\mathrm{Pb}\right)_{spl} = moles\left(^{205}\mathrm{Pb}\right)_{spl} \cdot \left[ \left(\frac{^{206}\mathrm{Pb}}{^{205}\mathrm{Pb}}\right)_{fc} - \left(\frac{^{206}\mathrm{Pb}}{^{205}\mathrm{Pb}}\right)_{tr} \right] - moles\left(^{206}\mathrm{Pb}\right)_{tpb} \tag{3}$$

where $fc$ denotes a measured, fractionation-corrected ratio, $tr$ the tracer, $spl$ the sample, and $tpb$ the total procedural blank.

However, if the tracer IC was on the measured tracer-blank mixing line, but its location was chosen incorrectly, then its (incorrect) IC could be expressed as

$$\left(\frac{^{206}\mathrm{Pb}}{^{205}\mathrm{Pb}}\right)' = \left(\frac{^{206}\mathrm{Pb}}{^{205}\mathrm{Pb}}\right)_{tr} + \left(\frac{^{206}\mathrm{Pb}}{^{204}\mathrm{Pb}}\right)_{bl} \cdot (\Delta\tau) \tag{4}$$

where $(\Delta\tau)$ is proportional to the incorrect displacement along the tracer-blank mixing line. Calculating equations (2) and (3) with $(^{206}\mathrm{Pb}/^{205}\mathrm{Pb})tr'$, the resulting difference between the calculated values of $moles(^{206}\mathrm{Pb})_{spl}$ is

$$\Delta\, moles\big(^{206}\mathrm{Pb}\big)_{spl} = \big[moles(^{205}\mathrm{Pb})_{spl} - moles(^{205}\mathrm{Pb})_{tpb}\big] \cdot (\Delta\tau) \cdot \left(\frac{^{206}\mathrm{Pb}}{^{204}\mathrm{Pb}}\right)_{bl} \tag{5}$$

According to equation (5), an incorrect choice of the location for the tracer IC on the tracer-blank mixing line incurs an error that is proportional to the difference in the moles of $^{205}$Pb added to the sample and to the total procedural blank, or for several total procedural blanks, their mean. If the same quantity of tracer is used for spiking the total procedural blank measurements and the samples, then the first term on the right-hand side of equation (5) approaches zero, and the arbitrary choice of the location of the tracer IC on the tracer-blank mixing line will have a minimal affect the reduced data.

## 4. A Model for Determining the U 'Double Spike IC' and Uncertainty

The U isotopic composition of the tracer was determined using the critical mixture approach (Krogh, 1964; Hofmann, 1971; Condon et al., in review) using the uranium isotopic reference materials CRM U500 and CRM 112a as end-member mixture components. Although the critical mixture concept was formulated using a linear fractionation law, it applies to an exponential fractionation law as well. The trend predicted by variable-magnitude exponential fractionation, which deviates from its linear approximation less than 10ppm over observed isotopic fractionation values, is very close to parallel to the mixing line in the vicinity of the critical mixture.

In the same way that data from several constraints on the IC of Pb reference materials were confederated to calculate the best estimate of several model parameters simultaneously in Section 2.1, many measurements of the tracer, measured both on its own and mixed in critical mixture proportions can be combined to constrain the U IC of the tracer. The solution and minimization take a similar form.

### *4.1. Algorithm and Results*

To solve for the U IC of ET(2)535, we use multiple critical mixture IC measurements with both SRM U500 and CRM 112a as isotopic reference materials, as well as several measurements of pure tracer alone. All U loads were estimated to be 500 ng, and U blanks 0.1 pg, which is assigned a 100% prior relative uncertainty to account for loading blank mass variability. The $^{238}$U/$^{235}$U of the blank is estimated to be 137.82, an average of terrestrial sources relative to IRMM 3636 (Hiess et al., 2012) with no uncertainty assigned because the magnitude of the blank subtraction is nearly negligible.

As with the Pb reference material inter-calibration, a least squares inverse solution to the large system of overdetermined equations in (B.13) created by several measurements is reached by a

preconditioned gradient descent method. The unknown variables the U IC of the tracer, as well as the sample/spike ratio of each measurement and the magnitude of isotopic fractionation are assigned large prior relative uncertainties. This analysis utilizes 14 measurements of SRM U500, 12 of CRM 112a, and 7 of pure tracer made at NIGL and MIT.

The uncertainties in the ICs of the U reference materials used in the critical mixtures are treated as systematic uncertainties. To determine their contribution to the total uncertainty in the tracer U IC, a Monte Carlo algorithm is employed, which is used to test the assumption that the system is locally linear at its least-squares solution. Monte Carlo realizations of the $^{238}U/^{235}U$ of SRM U500 and CRM 112a are generated by a pseudorandom number generator with the distribution given in Tables 1 and 2, and the uncertainty of each realization is assumed to be infinitesimally small. The least squares solution is then calculated for $10^4$ Monte Carlo realizations of the U reference material ICs, and their variability represents the systematic uncertainty contribution from the U reference material ICs. This estimate is combined with the measurement uncertainties derived by solving the system at the maximum likelihood estimate of the U reference material ICs to calculate the total uncertainty in the U IC of the tracer (equation A.3).

The results of the critical mixtures experiment are presented in Table 8. The null hypothesis that the Monte Carlo realizations used to calculate the systematic uncertainty contribution are normally distributed is accepted by a K-S test with a p-value of 0.9 for both the $^{233}U/^{235}U$ and $^{238}U/^{235}U$ of the tracer. This result permits addition of the measurement and systematic uncertainty covariance matrices, the multivariate analog of quadratic uncertainty addition.

### *4.2. Correlation with Sample $^{238}U/^{235}U$*

In an important development for high-precision U-Pb geo- and cosmochronology, the $^{238}U/^{235}U$ of samples has been found to vary beyond measurement precision (Condon et al., 2010; Hiess et al., 2012; Stirling et al., 2007; Weyer et al., 2008). In order to determine the $^{238}U/^{235}U$ of each sample, its IC can be measured against IRMM 3636. Thus, in the same way that the U IC of the tracer can be traced to the IC of IRMM 3636, so can a precisely determined $^{238}U/^{235}U$ value, and the uncertainties of both are therefore correlated. Since uncertainties in both the tracer and sample U IC are used to determine the total uncertainty budget for a U-Pb date, this correlation must be calculated and included in the uncertainty propagation.

To assess their degree of correlation, the derivative of the mean $^{238}U/^{235}U$ for the sample and the tracer IC must be evaluated relative to the IC of IRMM 3636. For the specific accessory phases measured in Hiess et al. (2012), as well as the reported average zircon $^{238}U/^{235}U$ of $137.817 \pm 0.045$, these derivatives are found in the Supporting Online Materials. For the tracer U ratios, the derivatives are reported in Table 7, along with the derivatives of the tracer $^{235}U/^{205}Pb$ derived in Section 6. The covariance between the tracer and sample ICs can be calculated with a Jacobian matrix, or matrix of partial derivatives, and a covariance, using the equation

$$\mathbf{\Sigma}_{ts} = J^{\mathsf{T}} \mathbf{\Sigma}_{3636} J \tag{6}$$

where $J$ is a Jacobian matrix that contains the derivatives of the tracer and sample IC with respect to the IC of IRMM 3636, like that presented in Table 7, and $\mathbf{\Sigma}_{3636}$ is the covariance matrix for the IRMM 3636 IC. The resulting tracer-sample covariance matrix $\mathbf{\Sigma}_{ts}$ contains, as its off-diagonal components, covariance terms that relate the tracer and sample IC, which can be used in a U-Pb uncertainty propagation algorithm such as McLean et al. (2011).

### *4.3. Sample Fractionation Correction with a $^{233}U$-$^{235}U$ Tracer*

The true IC of the mixture is known to lie on a mixing line between the ICs of the tracer and sample, both of which are required for this calculation. For a finite fractionation factor $\beta$, the measured IC lies off of the mixing line, along a fractionation line from the true IC on the mixing line to the measured IC of the sample. Geometrically, fractionation correction entails finding the point on the mixing line whose fractionation line goes through the measured datum.

However, at the critical mixture IC used above, the fractionation line is parallel to the mixing line. Any error in the measurement or IC of the sample or tracer (even within arbitrarily small uncertainties) will result in a discrepancy between the mixing line and the measured data that cannot be corrected back to the mixing line along the parallel fractionation line. For measured ICs close to the critical mixture IC, fractionation lines are sub-parallel to the mixing line, and small errors (for instance, within measured uncertainties), can result in large, erroneous extrapolation distances back to the mixing line. For this reason, $^{233}$U-$^{235}$U tracers are not optimized for ICs near the critical mixture, and the $^{233}$U/$^{235}$U of the mixture should be chosen to avoid these sample-tracer ratios. For ET(2)535, uranium ICs near the critical mixture occur for very young under-spiked samples. For example, a 3 Ma sample with a $^{206}$Pb/$^{205}$Pb near 4.25 yields measured $^{238}$U/$^{235}$U ratios near 55, magnifying small errors in the measurement or estimate of the sample $^{238}$U/$^{235}$U. The simplest practical solution is to disregard the double-spike fractionation determination and instead use an average U fractionation value based on past determinations with smaller $^{238}$U/$^{235}$U values.

A perceived weakness of the 'hybrid' $^{233}$U-$^{235}$U tracer is that it cannot simultaneously be used to determine the $^{238}$U/$^{235}$U of the sample, as it instead relies upon a presumed value for this ratio. For routine U-Pb geochronologic analyses, however, there is not enough uranium available to measure the small $^{235}$U abundance with sufficient precision to detect the epsilon-level natural variation in $^{238}$U/$^{235}$U. For instance, the measurements presented in Hiess et al. (2012) comprise weighted means of multiple microgram-mass uranium samples, whereas routine U-Pb geochronology involves samples with a few nanograms or less.

## 5. U/Pb Ratios of the Gravimetric Solutions

In order to determine the U/Pb ratio of each gravimetric solution, three aliquots of high-purity Pb and U reference materials were weighed then dissolved in acid in three independent labs, creating solutions whose U-Pb ratios are gravimetrically calibrated. The uncertainty in the U/Pb ratio of each gravimetric solution is a function of the uncertainties in the masses of the reference materials and their purities. The procedures by which the three gravimetric solutions were mixed in independent laboratories is included in (Condon et al., in review).

The $^{235}$U/$^{205}$Pb and $^{202}$Pb/$^{205}$Pb ratio of the tracer were determined against three separate gravimetric solutions for several reasons. First, the uncertainties due to the mass measurements of the Pb and U metal used to make the solutions, as well as their purities, are major contributions to the uncertainty in the U/Pb ratio of the gravimetric solutions, and therefore the U/Pb ratio of the tracer. Evaluating the mean tracer U/Pb ratio over multiple independently mixed solutions averages out some of this uncertainty. Also, the different $^{206}$Pb/$^{238}$U ratios of the solutions, ranging from 0.094 for the RP solution to 0.017 for the ET solution, allow for varied sample/tracer ratios for each element when mixed with a tracer with a constant $^{235}$U/$^{205}$Pb. Using multiple sample/tracer

ratios and Pb and U ratios for internal fractionation correction provides an additional check for internal consistency between results.

### *5.1. Uncertainty in Mass Determinations*

The masses of the Pb and U reference materials were determined before the metals were dissolved to create the gravimetric solutions. Although care was taken to remove oxidation and surface contamination before weighing on precise balances, each mass measurement has finite uncertainty. Because the ultimate parameter of interest is the U/Pb ratio of the solutions, any scale bias that is linearly proportional to the measured mass will divide out. Thus we propagate only the uncertainty determined from the reproducibility of successive measurements of calibration weights and the Pb and U metals. Additional corrections were made to account for buoyancy effects, but the magnitude and systematic nature of these corrections resulted in a negligible contribution to the U/Pb ratio uncertainty.

### *5.2. Uncertainty in Purity of Pb Isotopic Reference materials*

Although the purity, or the assay, of both NBS reference and assay materials and the Puratronic Pb are certified, these measurements are often dated, contain no supporting information, and are quoted with conservative uncertainties (e.g. ">99.9%" for NBS 981 and 982). A purity quotation in this form is unhelpful because there is no expected value or probability density function (pdf) from which to construct confidence intervals or perform uncertainty analysis. In order to better quantify the purity of the Pb isotopic reference materials used here, the purities of NBS 981, 982, 983, and Puratronic Pb were measured by glow discharge mass spectrometry at the GD-MS facility of the National Research Council (NRC) of Canada. The raw data appears in the electronic supplement of Condon et al. (in review).

Elemental concentrations from GD-MS are reported in two formats. If a significant isobaric interference exists at the same mass to charge ratios as the element of interest, observed as an elevated baseline in the mass scan, then its concentration is reported as <X ppb. This result may reasonably be interpreted as a uniform probability distribution function with limits at zero and X ppb. If no significant isobaric interference is detected, then the concentration is reported without the less than symbol, and repeated reference material analyses indicate the concentration of each element may be represented as with a triangular pdf (Fig. 7). The triangular distribution has a mean and mode at the stated concentration, and upper and lower limits at ±50% of the measured value.

The purity of each Pb reference material is defined as the difference between unity and the sum of all the impurities. Since the pdfs for the impurities are not Gaussian, uncertainty propagation by quadratic summation is not applicable. Instead, we employ a Monte Carlo approach, where a randomly generated realization from the pdf of each element's concentration is summed to produce a model value for the total impurity concentration. This process was iterated $10^7$ times for each reference material, and the resulting distribution of purities, normalized to unity, is an accurate estimate of the pdf for the purities. The pdf is closely approximated by a histogram of the Monte Carlo realizations with small bin sizes, illustrated in Figure 7. Because the pdfs of each elemental concentration are symmetric, the pdf of the total impurities is also symmetric, and the maximum likelihood estimate and 95% confidence interval for each reference material may be expressed as a symmetric range about the mean, listed in Table 9.

### 5.3. Purity of U Isotopic Reference materials

The purities of the U reference materials used to make the gravimetric solutions, CRM 112a and CRM 115, have been recently certified to significantly higher precision than the older Pb reference materials. In a Sept. 2010 revision of the CRM 112a certificate of analysis by the New Brunswick Laboratory, the total impurity concentration is reported as 223 $\mu$g/g U, which equates to a purity of 0.999777 g U/g metal, and the total uncertainty in the assay is reported as 0.00006 g U/g metal, expressed as an approximate 95% confidence interval calculated with a $k = 2$ coverage factor. The coverage factor and confidence interval width together imply that the modeled distribution is Gaussian, with a standard deviation of 0.00003 g U/g metal. Likewise, the CRM 115 purity is reported (April 2012 certification) as $0.999770 \pm 0.000046$, with the same coverage factor and stated confidence interval, translating to a standard deviation of 0.000023.

### 5.4. Gravimetric U/Pb ratio

The U/Pb ratio of the gravimetric solution is most conveniently expressed as its $^{206}$Pb/$^{238}$U ratio, which can be determined from the total moles of each isotope present. The moles of $^{206}$Pb in the gravimetric solution is

$$moles(^{206}\mathrm{Pb}) = \frac{mass(\mathrm{Pb}_{grav}) \cdot purity(\mathrm{Pb}_{grav})}{M_{204} \cdot \left(\frac{^{204}\mathrm{Pb}}{^{206}\mathrm{Pb}}\right)_{gr} + M_{206} + M_{207} \cdot \left(\frac{^{207}\mathrm{Pb}}{^{206}\mathrm{Pb}}\right)_{gr} + M_{208} \cdot \left(\frac{^{208}\mathrm{Pb}}{^{206}\mathrm{Pb}}\right)_{gr}} \tag{7}$$

and likewise the moles of $^{238}$U in the solution is

$$moles(^{238}\mathrm{U}) = \frac{mass(\mathrm{U}_{grav}) \cdot purity(\mathrm{U}_{grav})}{M_{234} \cdot \left(\frac{^{234}\mathrm{U}}{^{238}\mathrm{U}}\right)_{gr} + M_{235} \Big/ \left(\frac{^{238}\mathrm{U}}{^{235}\mathrm{U}}\right)_{gr} + M_{238}} \tag{8}$$

The $^{206}$Pb/$^{238}$U ratio of the gravimetric solution is simply the quotient of equations (7) and (8).

## 6. Gravimetric-Tracer Mixtures

In order to determine the U/Pb ratio of the tracer, expressed as the ratio of two of its enriched isotopes, $^{235}$U/$^{205}$Pb, as well as its $^{202}$Pb/$^{205}$Pb, the tracer was mixed with the series of three gravimetric solutions described in Section 5.2. Measuring the U/Pb ratio of the tracer against the known U/Pb ratio of a gravimetric solution is the inverse of measuring a sample U/Pb ratio with the tracer: the known ICs of the gravimetric solution Pb and U components can be used to fractionation-correct the measured Pb and U tracer/sample ratios, then the known U/Pb ratio of the gravimetric solution is used to determine the U/Pb ratio of the tracer. The small contributions of laboratory blank and non-enriched tracer isotopes complicate the calculation, but as with the Pb reference material inter-calibration and U critical mixtures, the resulting mixture can be represented by a system of non-linear equations, and the best estimate of the tracer parameters reached with a non-linear least squares approach.

### 6.1. Algorithm and Results

A total of 46 paired Pb and U measurements were analyzed at NIGL and MIT: 19 with the RP solution, 14 with ET, and 13 with JMM. Of these mixtures, 15 used ET2535 and 31 used ET535. The Pb and U for each mix were loaded together on Re filaments, with the Pb run as a metal and U as $UO_2^+$ polyatomic ion, described in Condon et al. (in review). Between 100 and 600 independent isotope ratios were measured for each Pb and U solution, provided in the electronic supplement. The mean of each block, defined as 20 consecutive ratio measurements, was evaluated along with the multivariate analog of its squared standard error, the covariance matrix for all isotope ratios divided by $n - 1 = 19$ degrees of freedom. A total of 212 blocks of Pb were measured with ET2535, 579 with ET535, and 644 blocks of U, for a total of $212 \times 4 + 579 \times 3 + 644 \times 2 = 3873$ ratio means.

The most important model parameters in the system described above are the $^{235}U/^{205}Pb$ and the $^{202}Pb/^{205}Pb$ of the tracer. In order to solve for these, the following variables must be determined for each analysis: the mass-independent fractionation parameters $\gamma_{205}$ and $\gamma_{207}$, and the ratio of gravimetric solution to tracer, parameterized by $^{238}U_{gr}/^{235}U_{tr}$. These variables are assigned initial values based on a linearized solution to the model and assigned diffuse priors. Additionally, the $^{207}Pb/^{206}Pb$ and $^{208}Pb/^{206}Pb$ of the laboratory blank are known to vary between loads, along with the mass of the Pb and U blanks themselves.

The Pb blank IC for each bead is assigned an IC calculated using data from MIT and NIGL, and its the prior uncertainty derived in Section 3. The Pb and U blank mass initial values are 0.3 and 0.1 pg, respectively, and given a 100% relative uncertainty, which allows the least-squares algorithm to determine the blank mass for each load that best fits the data. To ensure that tracer IC estimates are not dependent on the choice of Pb blank IC, full calculations were performed with a range of ICs measured at MIT and NIGL. The discrepancies were well within our reported numerical precision, smaller than the significant digits reported in data tables herein. Finally, an initial value for the magnitude of isotopic fractionation for each block, $\beta_j^i$, was estimated for each Pb and U block using a simple linearized model and assigned a diffuse prior. In total, there are 1759 unknowns constrained by 3873 isotope ratio measurements, so the system itself is overdetermined.

For the gravimetric mixtures, the uncertainties in the gravimetric solution Pb and U ICs, the tracer minor isotope IC, and the U/Pb ratios of the gravimetric solutions are all treated as systematic uncertainties, since they are not expected to vary from mixture to mixture. To propagate their uncertainties, Monte Carlo simulations of each were created using the probability distribution functions for the Pb and U ICs of the reference materials, as well as their purities and mass determinations. The non-linear least squares model with the data and model parameters described above was solved for 2000 Monte Carlo realizations of these systematic effects.

Monte Carlo realizations of the gravimetric solution $^{206}Pb/^{238}U$ values include the non-Gaussian probability distribution functions for the Pb purities derived from the GD-MS measurements, and thus themselves cannot be assumed to be perfectly normally distributed. Testing the distribution of the Monte Carlo realizations of the $^{235}U/^{205}Pb$ and the $^{202}Pb/^{205}Pb$ of the tracer, the null hypothesis that the distributions are Gaussian is accepted with a p-value of 0.89 and 0.97, respectively. Although the distribution of the Pb reference material purities, which are included in this calculation, are not Gaussian, they are overwhelmed by other uncertainties, notably the $^{208}Pb/^{206}Pb$ of NBS 981 and the $^{233}U/^{236}U$ of IRMM 3636, both of which are assumed to be normally distributed. Therefore, the systematic uncertainties may be combined using equation (A.2) with the measurement uncertainties for the $^{235}U/^{205}Pb$ and the $^{202}Pb/^{205}Pb$ using equation (A.3). The results are given in Table 10.

## 7. Discussion: Impact of the Tracer Calibration model on U-Pb dates

The highest precision dates produced by U-Pb geochronology, used to calibrate the geologic timescale from the Paleozoic through the Cenozoic, are $^{206}Pb/^{238}U$ dates. For samples younger than about 500 Ma, both $^{238}U$ and $^{206}Pb$ are more abundant than $^{235}U$ and $^{207}Pb$, and thus the uncertainty in the $^{207}Pb/^{206}Pb$ date is dominated by the blank correction to the less abundant amount of ingrown $^{207}Pb$. Analysis of the total contribution of the tracer calibration uncertainties to the uncertainty in a $^{206}Pb/^{238}U$ date is performed with a simplified data reduction scheme. The only isotopes considered are $^{202}Pb$, $^{205}Pb$, and $^{206}Pb$ along with $^{233}U$, $^{235}U$, and $^{238}U$. Using the tracer parameters calculated above along with reasonable sample/tracer ratios and a range of frequently observed fractionation factors, hypothetical measured ratios corresponding to a range of dates were calculated. For instance, a 100 Ma sample with a sample $^{238}U/^{235}U$ ratio of 137.814 and a sample/tracer ($^{238}U_{spl}/^{235}U_{tr}$) ratio of 1 will have a measured $^{206}Pb/^{205}Pb$ ratio of about 1.56 and $^{238}U/^{235}U$ ratio of 0.988, assuming typical magnitudes of isotopic fractionation of 0.2% per u for Pb and 0.1% per u for U.

Using the measured values calculated in this way, a $^{206}Pb/^{238}U$ ratio can be calculated by fractionation-correcting the measured $^{206}Pb/^{205}Pb$ and $^{238}U/^{235}U$ ratios using the $^{202}Pb/^{205}Pb$ and $^{233}U/^{235}U$ ratios, then utilizing the isotope dilution formula

$$\left(\frac{^{206}Pb}{^{238}U}\right)_{spl} = \left(\frac{^{206}Pb}{^{205}Pb}\right)_{fc} \Bigg/ \left[\left(\frac{^{238}U}{^{235}U}\right)_{fc} \cdot \left(\frac{^{235}U}{^{205}Pb}\right)_{tr}\right] \tag{9}$$

where $fc$ denotes a measured, fractionation-corrected ratio. The $^{206}Pb/^{238}U$ can then be used to calculate a date.

There are three pertinent tracer parameters whose uncertainty must be considered: the $^{202}Pb/^{205}Pb$, $^{233}U/^{235}U$, and $^{235}U/^{205}Pb$ ratios. Because both the $^{235}U/^{205}Pb$ and the $^{202}Pb/^{205}Pb$ derive much of their uncertainty from the *a priori* uncertainty of the $^{208}Pb/^{206}Pb$ of NBS 981, their uncertainties are highly correlated. The result is a relatively large, negative correlation coefficient, which indicates that a positive error in the $^{202}Pb/^{205}Pb$ is likely correlated with a negative error in the $^{235}U/^{205}Pb$, and vice versa. The two effects partially cancel one another: a higher $^{202}Pb/^{205}Pb$ results in a smaller fractionation correction and therefore less apparent $^{206}Pb$, but the lower $^{235}U/^{205}Pb$ increases the apparent $^{206}Pb/^{238}U$ (equation 9). Likewise, the $^{235}U/^{205}Pb$ and $^{233}U/^{235}U$ both depend on the $^{233}U/^{236}U$ of IRMM 3636, and therefore their uncertainties are also correlated. In this case, the correlation is positive, and an increase in the tracer $^{233}U/^{235}U$ results in a smaller fractionation correction and less apparent $^{238}U$, which is partially offset by the larger likely $^{235}U/^{205}Pb$.

In this way, the uncertainty correlations between the $^{235}U/^{205}Pb$ and both the $^{202}Pb/^{205}Pb$ and $^{233}U/^{235}U$ act to decrease the effective uncertainty in the $^{206}Pb/^{238}U$ date. As Figure 8 shows, ignoring all covariance terms between the tracer ratios results in an overestimation of the tracer uncertainty contribution by a factor of almost two. The only published U-Pb uncertainty propagation algorithm to include the required covariance terms is (McLean et al., 2011), which permits uncertainty correlations between all tracer parameters. Current version of the ICs and uncertainties of both ET535 and ET2535 are available for download into the associated U-Pb_Redux software package through the EARTHTIME initiative.

## 8. Conclusions

Correct tracer uncertainty propagation is essential to accurate, precise U-Pb isotope dilution geochronology. This contribution, combined with the data and metrological traceability outlined in Condon et al. (in review) presents a measurement model that links first-principles mass and purity measurements to a complete description of the EARTHTIME ($^{202}$Pb-$^{205}$Pb-$^{233}$U-$^{235}$U) tracer isotopic composition, using a series of mixtures between the tracer and gravimetric solutions with known U/Pb ratios and isotopic compositions. The foundation of the tracer calibration depends upon two sets of measurements: the gravimetrically determined $^{208}$Pb/$^{206}$Pb of NBS 981 and the $^{233}$U/$^{236}$U of IRMM 3636, and the weights and purities of the three Pb reference materials and two U reference materials used to make three independently calibrated gravimetric solutions. Because the tracer ratios with the strongest influence on U-Pb dates, the $^{202}$Pb/$^{205}$Pb, $^{233}$U/$^{235}$U, and $^{235}$U/$^{205}$Pb ratios, are mutually dependent on the first-principles measurements, their uncertainties are significantly correlated. This correlation acts to decrease the overall uncertainty contribution to U-Pb dates due to tracer calibration.

The improvement presented here over the commonly assumed tracer calibration uncertainty of ca. 0.1% to <300 ppm represents a significant increase in the accuracy and transparency of U/Pb determinations and resultant calculation of U-Pb dates. Other labs using the same algorithms with calibration experiment underpinned by appropriate isotopic and assay reference materials should be able to collaboratively combine U-Pb data at the sub per-mil level, which approaches modern measurement uncertainties. The converse is also true: a precise tracer calibration is capable of revealing sub-per-mil variation between collaborating laboratories that may be due to previously unrecognized instrument calibration or laboratory blank biases. Finally, by establishing U-Pb dates (i.e., $^{206}$Pb/$^{238}$U and $^{207}$Pb/$^{235}$U) in an absolute reference frame, this tracer calibration combined with the $^{235}$U and $^{238}$U decay constant data (Jaffey et al., 1971) legitimizes further efforts at inter-calibrating the U decay constants (e.g. Schoene et al., 2006; Mattinson, 2010; Cheng et al., 2013) as well as the U-Pb system with other radio-isotopic dating systems through the analyses of assumed coeval geological materials (e.g. Nebel et al., 2011; Renne et al., 2010) and the accurate calibration of geologic time through U-Pb geochronology.

## Acknowledgements

This research was supported by NSF Award EAR 0451802 (the EARTHTIME project), NERC Fellowship NE/C517909/1, NERC grant NE/I013814/1, and NIGFSC award (IP/1028/0508). We thank Ralph Sturgeon for guidance interpreting glow discharge mass spectrometry data, and Yuri Amelin for kindly sharing Pb standard data.

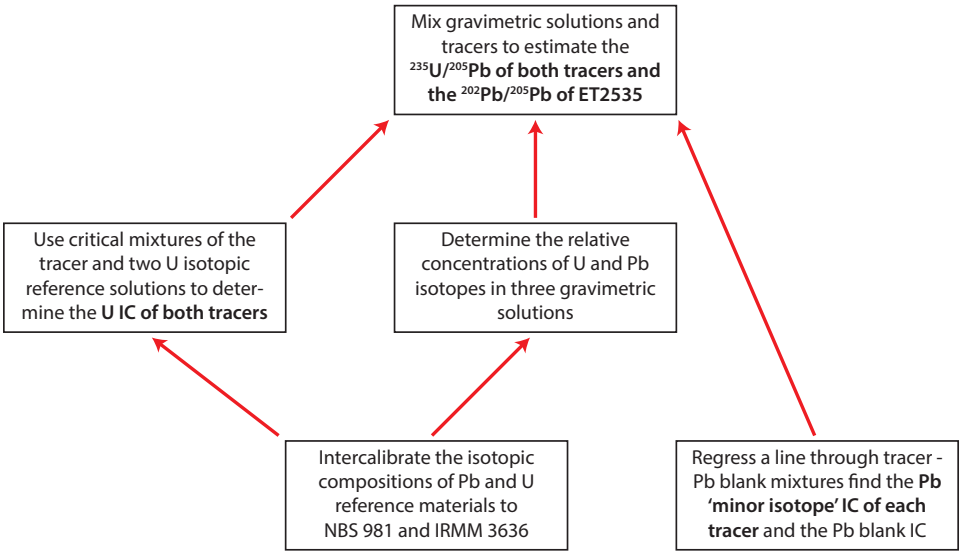


Figure 1: Flow diagram of U-Pb tracer calibration, which consists of five linked experiments that determine the isotopic and elemental composition (Pb IC, U IC, and Pb/U) of mixed U-Pb tracers. The flow proceeds from the bottom to the top of the figure.

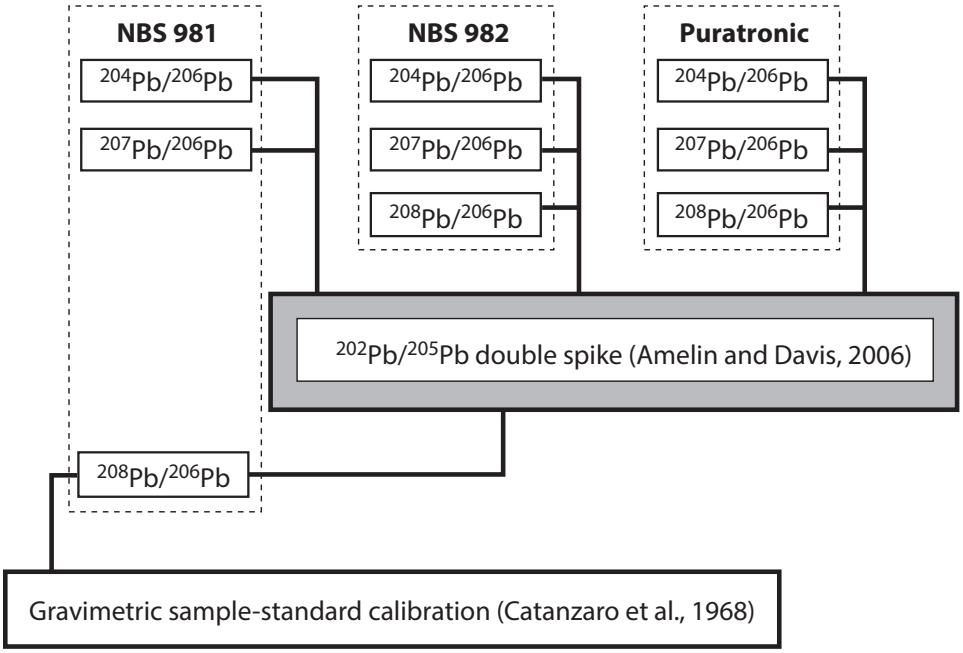


Figure 2: Diagram showing the traceability relationships between the isotopic compositions of the three inter-calibrated Pb reference materials. Note that the $^{208}Pb/^{206}Pb$ of NBS 981 is assumed to be $2.1681 \pm 0.0008$ ($2\sigma$), and all other measured isotopic compositions are derived relative to this value.

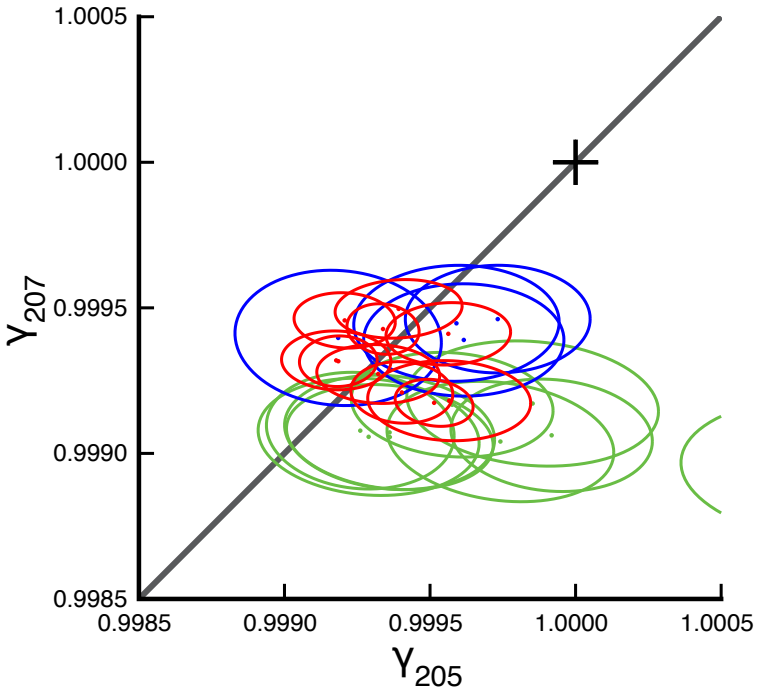


Figure 3: Measurements of the magnitude of MIF for the mixtures of Pb isotopic reference materials and a $^{202}$Pb-$^{205}$Pb tracer. The parameters $\gamma_{205}$ and $\gamma_{207}$ of McLean (2014) quantify the degree of mass-independent fractionation, empirically modifying the conventional exponential fractionation equation (B.4). Data is from Amelin and Davis (2006) along with newer measurements with the same tracer. The red data is from mixtures of NBS 981, green NBS 982, and blue Puratronic Pb. The black cross on the gray 1:1 line is the predicted behavior using a mass-dependent exponential fractionation law. Ellipses are $2\sigma$ or $\sim$86% confidence intervals, with all sources of uncertainty propagated.

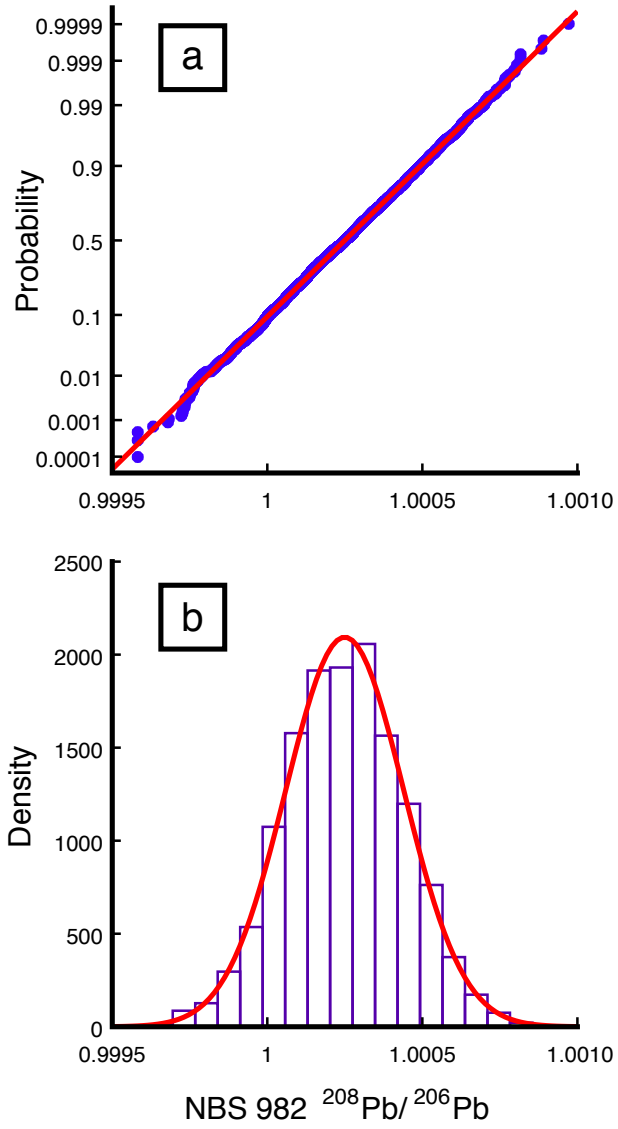


Figure 4: Five thousand Monte Carlo simulations of the effect of systematic uncertainties on the best-fit value of $^{208}$Pb/$^{206}$Pb of NBS 982. a) Probability plot of all Monte Carlo solutions. An ideal Gaussian distribution with the mean and standard deviation of the Monte Carlo solutions should plot on the diagonal red line. b) Histogram of Monte Carlo solutions with overlaid Gaussian distribution (red) with the observed mean and standard deviation. Both plots demonstrate that the Monte Carlo solutions are well-approximated by a Gaussian distribution, confirmed by a one-sided K-S test.

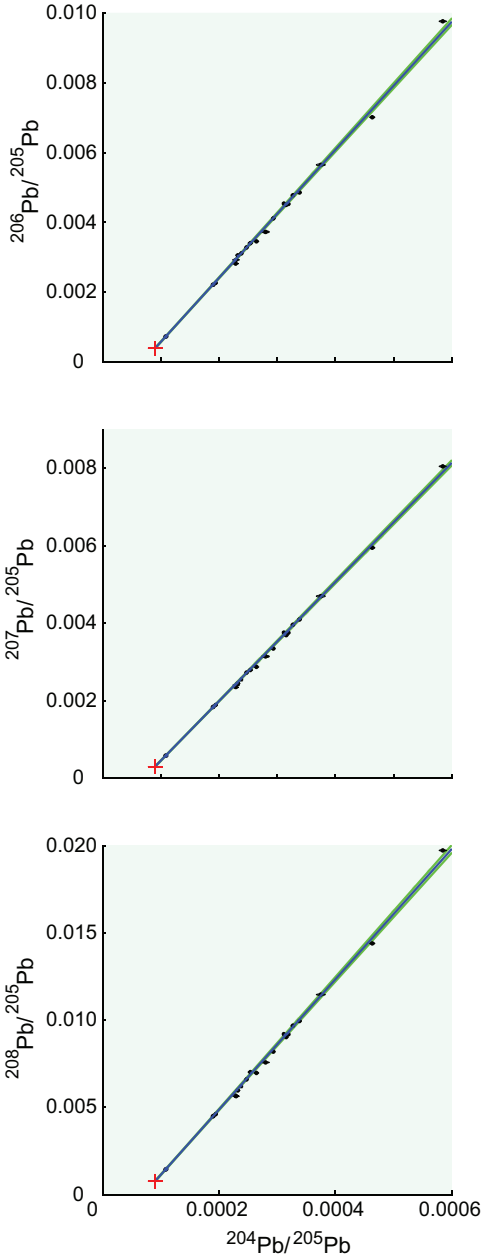


Figure 5: Results of multi-dimensional linear regression through the observed mixing line between ET535 and 22 total procedural Pb blank measurements. The best fit line is shown in blue, with its $2\sigma$ uncertainty envelope in green, and uncertainties in each data point are generally smaller than their marker size. The isotopic composition of ET535 is constrained to be on this line, contain less common Pb than the cleanest observed analysis, and have positive isotope ratios. Our estimate of the isotopic composition, shown in red, is therefore chosen to be halfway between the cleanest analysis and the location at which the mixing line leaves positive ratio space, with a $2\sigma$ uncertainty that spans this distance. The slope of the mixing line defines the average isotopic composition of the Pb blank: for instance, in the $^{206}Pb/^{205}Pb$ vs. $^{204}Pb/^{205}Pb$ projection of the four-dimensional line, the slope is the $^{206}Pb/^{204}Pb$ of the Pb blank.

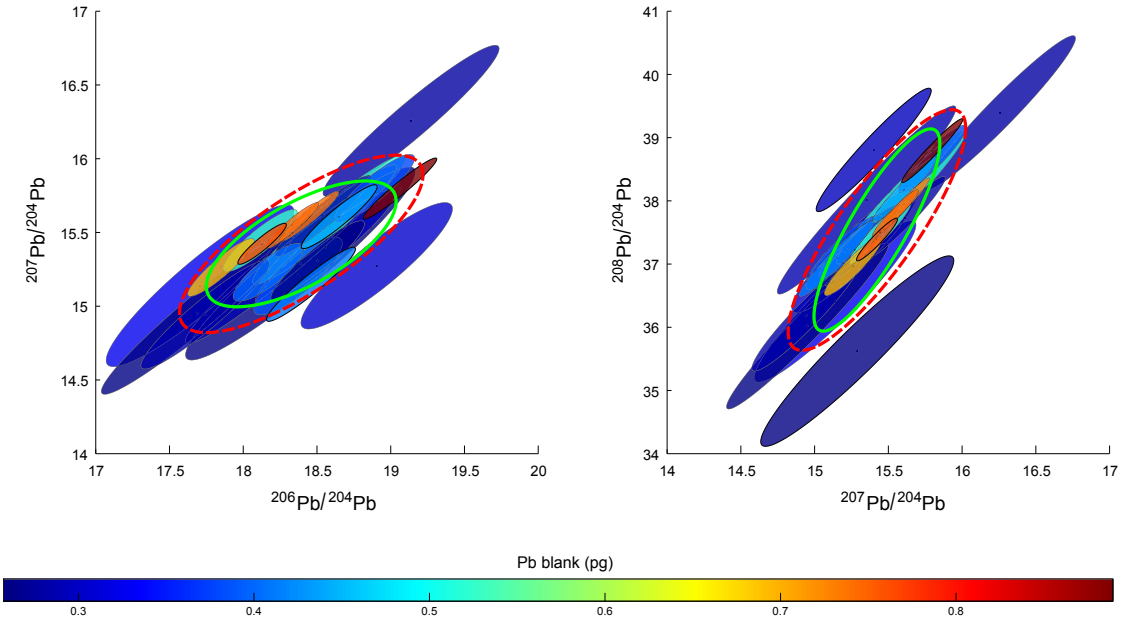


Figure 6: Measurements of the blank isotopic composition after subtracting the final tracer IC. All ellipses are $2\sigma$, or $\sim$86% confidence intervals, including ion counting and fractionation correction uncertainties, and color coded by the blank mass. The covariance ellipse for the discrete dataset of blanks is represented by the large red dashed ellipse, which does not account for the scatter in the blank ICs due to measurement uncertainty. The green ellipse is termed the overdispersion, which separates the positively correlated variability in the blank IC from the even more correlated measurement uncertainties (Vermeesch, 2010).

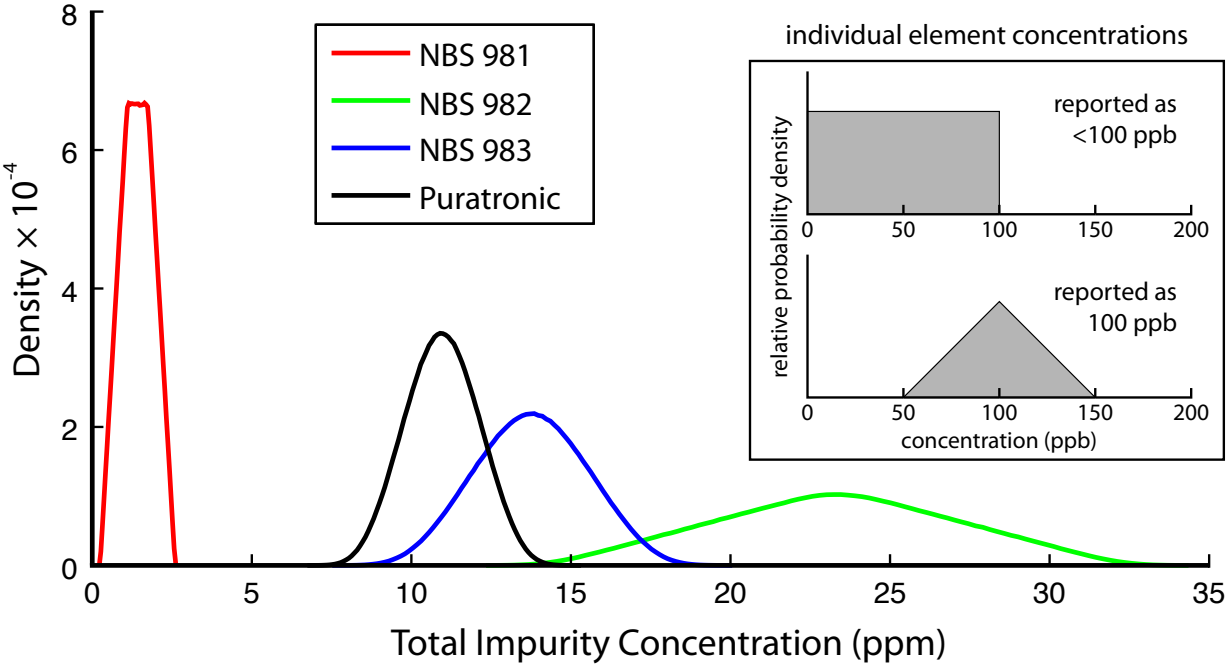


Figure 7: Probability distribution functions for the purity of four commonly used Pb reference materials, derived by summing elemental abundances measured by GD-MS. The inset shows the probability distribution functions assumed for the individual elements measured. In the presence of isobaric interferences, the true concentration is assumed to be between the measured value and zero, with equal relative probability along this interval. For a measurement free of isobaric interference, the true concentration is assumed to be within ±50% of the measured value, with the measured value being the most probable.

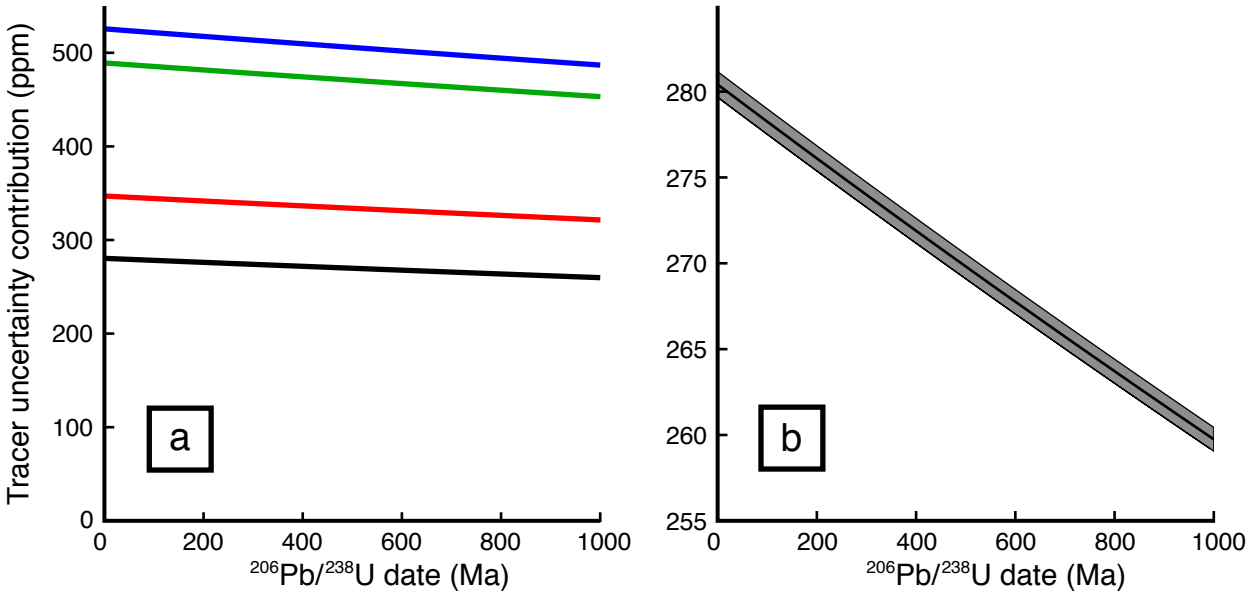


Figure 8: Relative uncertainty contribution ($2\sigma$, ppm) to the $^{206}Pb/^{238}U$ date from uncertainty in the tracer IC. a) The black line indicates the correct relative uncertainty contribution as a function of $^{206}Pb/^{238}U$ date. The red, green, and blue lines show the calculated uncertainty contribution if the covariance terms that belong to the tracer $^{233}U/^{235}U$, $^{202}Pb/^{205}Pb$, or all tracer variables, respectively, are neglected. b) The tracer contribution to the $^{206}Pb/^{238}U$ date uncertainty varies with the magnitude of isotopic fractionation. The shaded region encloses commonly observed values: Pb from 0.1 to 0.3% per u, and U from 0.0 to 0.2% per u.

Table 1: Weighted mean $^{238}U/^{235}U$ values and their random, and combined random and systematic uncertainties for the U isotopic standards CRM 112a, CRM 115, and CRM U500 used for tracer calibration. Reported ratios are all fractionation-corrected using the isotopic composition of IRMM 3636(a) (Verbruggen et al., 2008).

| | $^{238}U/^{235}U$ | $\pm 2\sigma$ [a] | $\pm 2\sigma$ [b] | MSWD | n (beads) |
|---|---|---|---|---|---|
| CRM 112a[c] | 137.841 | 0.011 | 0.024 | 1.4 | 7 |
| CRM 115 | 491.548 | 0.039 | 0.086 | 0.7 | 4 |
| CRM U500[c] | 0.999781 | 0.000077 | 0.00017 | 1.0 | 35 |

[a] propagating only components of uncertainty arising from random effects during measurement

[b] propagating components of uncertainty arising from systematic and random effects

[c] data from Condon et al. (2010)

Table 2: Matrix of correlation coefficients between the combined random and systematic uncertainties reported in Table 1

| | CRM 112a | CRM 115 | CRM U500 |
|---|---|---|---|
| CRM 112a | 1 | | |
| CRM 115 | 0.825 | 1 | |
| CRM U500 | 0.914 | 0.897 | 1 |

Table 3: Least squares solutions, random, and combined random and systematic uncertainties for the the Pb isotopic standards NBS 981, NBS 982, and Puratronic Pb used for tracer calibration, calculated with data reported in Amelin and Davis (2006)

| | | wtd. mean | $\pm 2\sigma$ [a] | $\pm 2\sigma$ [b] | n (blocks) |
|---|---|---|---|---|---|
| 981 | $^{204}Pb/^{206}Pb$ | 0.0590074 | 0.0000016 | 0.000022 | 160 |
| | $^{207}Pb/^{206}Pb$ | 0.914683 | 0.000011 | 0.00015 | |
| | $^{208}Pb/^{206}Pb$[c] | *2.1681* | – | *0.0008* | |
| 982 | $^{204}Pb/^{206}Pb$ | 0.0272058 | 0.0000021 | 0.000010 | 160 |
| | $^{207}Pb/^{206}Pb$ | 0.466967 | 0.000026 | 0.00008 | |
| | $^{208}Pb/^{206}Pb$ | 1.000249 | 0.000056 | 0.00039 | |
| Pur. | $^{204}Pb/^{206}Pb$ | 0.0548861 | 0.0000044 | 0.000021 | 36 |
| | $^{207}Pb/^{206}Pb$ | 0.856720 | 0.000046 | 0.00015 | |
| | $^{208}Pb/^{206}Pb$ | 2.10227 | 0.00011 | 0.00079 | |

[a] Propagating only components of uncertainty arising from random effects during measurement

[b] Propagating components of uncertainty arising from systematic and random effects

[c] Value from Catanzaro et al. (1968). All other isotope ratios are calculated relative to this value.

Table 4: Matrix of correlation coefficients between the combined random and systematic uncertainties in the Pb ICs used for tracer calibration. Correlation coefficients close to -1 or 1 indicate a high degree of correlation. The shared sources of systematic uncertainty largely responsible for the high correlation coefficients are the ratios being used for the fractionation correction.

| | | NBS 981 | | | NBS 982 | | | Puratronic Pb | | |
|---|---|---|---|---|---|---|---|---|---|---|
| | | $\frac{^{204}Pb}{^{206}Pb}$ | $\frac{^{207}Pb}{^{206}Pb}$ | $\frac{^{208}Pb}{^{206}Pb}$ | $\frac{^{204}Pb}{^{206}Pb}$ | $\frac{^{207}Pb}{^{206}Pb}$ | $\frac{^{208}Pb}{^{206}Pb}$ | $\frac{^{204}Pb}{^{206}Pb}$ | $\frac{^{207}Pb}{^{206}Pb}$ | $\frac{^{208}Pb}{^{206}Pb}$ |
| 981 | $^{204}Pb/^{206}Pb$ | 1 | | | | | | | | |
| | $^{207}Pb/^{206}Pb$ | -0.974 | 1 | | | | | | | |
| | $^{208}Pb/^{206}Pb$ | -0.990 | 0.991 | 1 | | | | | | |
| 982 | $^{204}Pb/^{206}Pb$ | 0.939 | -0.960 | -0.958 | 1 | | | | | |
| | $^{207}Pb/^{206}Pb$ | -0.875 | 0.809 | 0.846 | -0.753 | 1 | | | | |
| | $^{208}Pb/^{206}Pb$ | -0.965 | 0.919 | 0.950 | -0.883 | 0.943 | 1 | | | |
| Pur. | $^{204}Pb/^{206}Pb$ | 0.974 | 0.958 | -0.973 | 0.933 | -0.848 | -0.942 | 1 | | |
| | $^{207}Pb/^{206}Pb$ | -0.941 | 0.939 | 0.948 | -0.909 | 0.815 | 0.909 | -0.948 | 1 | |
| | $^{208}Pb/^{206}Pb$ | -0.982 | 0.975 | 0.988 | -0.947 | 0.850 | 0.950 | -0.986 | 0.961 | 1 |

Table 5: Results of linear fit for tracer - blank mixing line

| | ET535 | | ET2535 | | | Pb blank | |
|---|---|---|---|---|---|---|---|
| | value | $\pm 2\sigma$ | value | $\pm 2\sigma$ | | value | $\pm 2\sigma$ |
| $^{204}Pb/^{205}Pb$[a] | *0.000090* | *0.000018* | *0.000130* | *0.000050* | $^{206}Pb/^{204}Pb$ | 18.41 | 0.48 |
| $^{206}Pb/^{205}Pb$ | 0.00039 | 0.00034 | 0.00093 | 0.00092 | $^{207}Pb/^{204}Pb$ | 15.41 | 0.29 |
| $^{207}Pb/^{205}Pb$ | 0.00030 | 0.00028 | 0.00077 | 0.00077 | $^{208}Pb/^{204}Pb$ | 37.61 | 1.13 |
| $^{208}Pb/^{205}Pb$ | 0.00074 | 0.00070 | 0.0019 | 0.0019 | | | |

[a] This value is chosen arbitrarily to be half the distance from a null composition to the analysis with the highest ratio of tracer to blank (see Section 3.2).

Table 6: Correlation coefficient matrix for ET535 and loading blank Pb IC.

| | | ET535 Pb IC | | | | blank Pb IC | | |
|---|---|---|---|---|---|---|---|---|
| | | $\frac{^{204}Pb}{^{205}Pb}$ | $\frac{^{206}Pb}{^{205}Pb}$ | $\frac{^{207}Pb}{^{205}Pb}$ | $\frac{^{208}Pb}{^{205}Pb}$ | $\frac{^{206}Pb}{^{204}Pb}$ | $\frac{^{207}Pb}{^{204}Pb}$ | $\frac{^{208}Pb}{^{204}Pb}$ |
| ET535 | $^{204}Pb/^{205}Pb$ | 1 | | | | | | |
| | $^{206}Pb/^{205}Pb$ | 0.980 | 1 | | | | | |
| | $^{207}Pb/^{205}Pb$ | 0.989 | 0.992 | 1 | | | | |
| | $^{208}Pb/^{205}Pb$ | 0.974 | 0.987 | 0.992 | 1 | | | |
| blank | $^{206}Pb/^{204}Pb$ | 0 | -0.136 | -0.076 | -0.114 | 1 | | |
| | $^{207}Pb/^{204}Pb$ | 0 | -0.103 | -0.100 | -0.135 | 0.755 | 1 | |
| | $^{208}Pb/^{204}Pb$ | 0 | -0.099 | -0.086 | -0.156 | 0.729 | 0.864 | 1 |

Table 7: Derivatives of the U IC of ET(2)535 with respect to IRMM 3636, used to determine the covariance between a measured $^{238}U/^{235}U$ and the tracer, for propagating uncertainty in U-Pb dates.

| | | ET(2)535 | | |
|---|---|---|---|---|
| | | $\frac{^{233}U}{^{235}U}$ | $\frac{^{238}U}{^{235}U}$ | $\frac{^{235}U}{^{205}Pb}$ |
| IRMM3636 | $^{233}U/^{236}U$ | 0.6707 | 0.002907 | 99.79 |
| | $^{234}U/^{236}U$ | -.001262 | $4.209 \times 10^{-6}$ | -0.1951 |
| | $^{235}U/^{236}U$ | -0.8686 | 0.005051 | -121.8 |
| | $^{238}U/^{236}U$ | 0.4466 | -0.001505 | 68.93 |

Table 8: The U isotopic composition of ET(2)535 from the critical mixture experiment. The tracer was mixed with CRM 112a and SRM U500, whose ICs, uncertainties, and correlation coefficient are given in Section 2.2.

| | MLE | $\pm 2\sigma^a$ | $\pm 2\sigma^b$ | $\rho^c$ |
|---|---|---|---|---|
| $^{233}U/^{235}U$ | 0.995062 | 0.000009 | 0.00011 | -0.599 |
| $^{238}U/^{235}U$ | 0.00307993 | 0.00000064 | 0.00000080 | |

[a] propagating only components of uncertainty arising from random effects during measurement
[b] propagating components of uncertainty arising from systematic and random effects
[c] correlation coefficient between $^{233}U/^{235}U$ and $^{238}U/^{235}U$, with all uncertainties propagated

Table 9: Purities of Pb isotopic standards measured by glow discharge mass spectrometry, with estimated symmetric 95% confidence intervals

| | purity | 95%CI |
|---|---|---|
| NBS 981 | 0.9999986 | ±0.0000009 |
| NBS 982 | 0.9999767 | ±0.0000072 |
| NBS 983 | 0.9999862 | ±0.0000033 |
| Puratronic | 0.9999890 | ±0.0000047 |

Table 10: Results of the gravimetric solution - tracer mixtures.

| | MLE | $\pm 2\sigma^a$ | $\pm 2\sigma^b$ | $\rho^c$ |
|---|---|---|---|---|
| $^{202}Pb/^{205}Pb$ | 0.999239 | 0.000019 | 0.00053 | -0.915 |
| $^{235}U/^{205}Pb$ | 100.2329 | 0.0022 | 0.047 | |

[a] propagating only components of uncertainty arising from random effects during measurement
[b] propagating components of uncertainty arising from systematic and random effects
[c] correlation coefficient between $^{202}Pb/^{205}Pb$ and $^{235}U/^{205}Pb$, with all uncertainties propagated

## Appendix A. Application of inverse methods to tracer calibration

The parameters in the measurement model, such as the ICs and relative proportions of the tracer, isotopic reference materials, and blank, as well as the magnitude of isotopic fractionation, fall into three categories, depending on our state of knowledge at the beginning of the experiment. 1) Parameters measured by first principles, which underpin the tracer calibration. One example is the $^{233}U/^{236}U$ ratio of the U isotopic standard IRMM3636, whose value and uncertainty are traceable to first-principles measurements of mass (Verbruggen et al., 2008). Uncertainties in these parameters are not improved by the tracer calibration measurements, and can therefore be considered 'systematic.' 2) Parameters estimated from prior experience, such as the mass of the laboratory Pb blank in an analysis, which may be further constrained by the isotope ratio measurements. The values of these parameters are allowed to change within the available *a priori* constraints. 3) Free model parameters, such as the IC of the tracer, which have essentially no *a priori* information.

When formulated as an inverse problem (e.g. Tarantola and Valette, 1982a,b; Tarantola, 2005), the model may be expressed as $\mathbf{d} = \mathrm{G}(\mathbf{m})$, where $\mathbf{d}$ is a vector of data, in this case isotope ratio measurements, and $\mathrm{G}(\mathbf{m})$ is the function of the model parameters $\mathbf{m}$ that explains the measured data. A simple example would be fitting a line ($y = a\,x + b$) to $n$ measurements of a parameter ($y$) made at well-known positions ($x$) assumed to have zero uncertainty. In this case, the data vector $\mathbf{d}$ is a column vector containing the $n$ measured $y$-values $[y_1, y_2, \ldots y_n]$, and the model parameter vector $\mathbf{m}$ would have only two elements, $[a, b]$. The measurement model is the system of equations $y_i = a\,x_i + b$ that relates $\mathbf{d}$ to $\mathbf{m}$, so that $\mathrm{G}(\mathbf{m})$ is the linear function $\mathrm{G}([a, b]) = a\,x_i + b$.

### *Appendix A.1. Solving the Inverse Problem*

For the linked tracer calibration experiments, the $\mathrm{G}(\mathbf{m})$ functions found in equations (B.5), (B.13), and (B.8) are nonlinear, and because there are more measured isotope ratios in $\mathbf{d}$ than parameters to solve for in $\mathbf{m}$, the measurement model is overdetermined. There is no unique solution for the model parameters $\mathbf{m}$, but the best choice of the parameter values $\hat{\mathbf{m}}$ minimizes the misfit between the observed values of the isotope ratios ($\mathbf{d}$) on the left hand side of $\mathbf{d} = \mathrm{G}(\hat{\mathbf{m}})$ and the values predicted by best fit model parameters $\hat{\mathbf{m}}$ on the right-hand side. This 'misfit' is the weighted sum of two differences, the first between the data and the model predictions, $\mathbf{d} - \mathrm{G}(\hat{\mathbf{m}})$, which should fall within the uncertainties of the measured data, and the second between any prior constraints on the model parameters and the best fit values, $\mathbf{m_{prior}} - \hat{\mathbf{m}}$. These differences are weighted by the measured uncertainties for the data, embodied in the covariance matrix $\mathrm{C_D}$, and the *a priori* uncertainties in the model parameters, embodied in the covariance matrix $\mathrm{C_M}$. Free model parameters such as the isotopic composition of the tracer, considered unknowns, are given initial estimates with diffuse priors, or large initial uncertainties in $\mathrm{C_M}$ that ensure the initial estimate only negligibly affects the outcome.

The numerical value of the misfit is given by the objective function, whose minimum is the solution to the inverse problem (Tarantola, 2005),

$$S = \left(\mathbf{d} - \mathrm{G}(\hat{\mathbf{m}})\right)^{\mathsf{T}} \mathrm{C_D^{-1}} \left(\mathbf{d} - \mathrm{G}(\hat{\mathbf{m}})\right) + \left(\mathbf{m_{prior}} - \hat{\mathbf{m}}\right)^{\mathsf{T}} \mathrm{C_M^{-1}} \left(\mathbf{m_{prior}} - \hat{\mathbf{m}}\right) \tag{A.1}$$

where $\mathrm{C_D}$ and $\mathrm{C_M}$ are the covariance matrices of the measured data and the prior model parameter estimates, respectively. To minimize $S$, a stable linear preconditioned steepest descent method is employed (Tarantola, 2005). The algorithm calculates the gradient, or multi-dimensional direction in which the value of $S$ is most rapidly decreasing, then uses an estimate of the curvature of $S$

to determine a trial minimum value. At the trial minimum, a new gradient and curvature are estimated, and the procedure is iterated until convergence. The result is the maximum likelihood estimate of the model parameter values.

To evaluate the measurement uncertainties, or the joint conditional density function of the model parameters treated as unknowns given the best estimates of systematic variables, the overdetermined inverse problem was solved using near-zero prior uncertainties for the systematic variables. The measurement uncertainties are then estimated by approximating the system of equations with its Jacobian matrix evaluated at the best fit solution, denoted $G$. The matrix $G$ has a row for each measured isotope ratio and a column for each model parameter, and contains the derivative of each of the predicted measured isotope ratios with respect to each of the model parameters, so that $G(i, j) = (\partial \mathbf{d}_i / \partial \mathbf{m}_j)$. The posterior covariance matrix, which contains the measured uncertainties, is estimated using

$$\tilde{C}_{\mathrm{M}}^{meas} = \mathrm{C_M} - \mathrm{C_M}\, G^{\mathsf{T}} \left( G\, \mathrm{C_M}\, G^{\mathsf{T}} + \mathrm{C_D} \right)^{-1} G\, \mathrm{C_M} \tag{A.2}$$

which can be derived from equation (A.1), the objective function (Tarantola, 2005).

*Appendix A.2. Evaluating Systematic Uncertainties*

In order to evaluate the component of uncertainty arising from systematic effects, the entire nonlinear inverse problem can be solved for $M$ Monte Carlo realizations of the systematic parameters, created with a pseudorandom number generator to have the desired probability density function, here a multivariate Gaussian. The value of $M$ used for the inverse problems described here ranges from $10^4$ to $10^7$, depending on the computational difficulty of the calculation. The systematic parameters, such as the assumed $^{208}\mathrm{Pb}/^{206}\mathrm{Pb}$ ratio of NBS 981, can either be given infinitesimally small prior uncertainties to ensure that the model converges to the input value, or can be omitted from $\mathbf{m}$ entirely.

For the free model parameters treated as unknowns, the distribution of the M resulting solutions defines the probability distribution of the model parameters resulting from the input systematic uncertainties. Because the model is nonlinear, even if the uncertainties in the measured data and systematic variables all have Gaussian distributions, the calculated uncertainties in the other output model parameters, such as the $^{235}\mathrm{U}/^{205}\mathrm{Pb}$ of the tracer, may be significantly non-Gaussian. The departure from the normal distribution depends on both the degree of non-linearity of the system at the value of the solution and the size of the input uncertainties. Solving the least squares system for many Monte Carlo realizations of the systematic variables provides a way to evaluate the probability distribution of the output model parameters without assuming that the model is locally linear. The normality of the Monte Carlo-modeled solutions can be checked by plotting the data as a histogram or a Q-Q plot, or with a Kolmogorov-Smirnov (K-S) test, which compares the observed Monte-Carlo distribution with the theoretically predicted normal distribution with the same mean and standard deviation.

If the probability distributions of the free model parameters from the $M$ Monte Carlo solutions are confirmed to be normally distributed, they can be estimated by evaluating the mean and covariance matrix of the $M$ estimates of $\hat{\mathbf{m}}$, denoted $\tilde{C}_{\mathrm{M}}^{sys}$. The total systematic and measurement uncertainty can then be expressed as the sum of the measured and systematic covariance matrices:

$$\tilde{C}_{\mathrm{M}}^{tot} = \tilde{C}_{\mathrm{M}}^{meas} + \tilde{C}_{\mathrm{M}}^{sys} \tag{A.3}$$

## Appendix B. Measurement models

### *Appendix B.1. Pb Isotope Standards Inter-calibration Model*

To inter-calibrate the Pb isotopic reference materials against a $^{202}Pb/^{205}Pb$ tracer, while monitoring the effect of a $BaPO_2$ isobaric interference, six masses must be measured. The contributions to each measured mass may be broken down as follows,

$$\begin{aligned}
201_{tot} &= {}^{201}BaPO_2 \\
202_{tot} &= {}^{202}Pb_{tr} + {}^{202}BaPO_2 \\
204_{tot} &= {}^{204}Pb_{gr} + {}^{204}Pb_{bl} + {}^{204}Pb_{tr} + {}^{204}BaPO_2 \\
205_{tot} &= {}^{205}Pb_{tr} + {}^{205}BaPO_2 \\
206_{tot} &= {}^{206}Pb_{gr} + {}^{206}Pb_{bl} + {}^{206}Pb_{tr} \\
207_{tot} &= {}^{207}Pb_{gr} + {}^{207}Pb_{bl} + {}^{207}Pb_{tr} \\
208_{tot} &= {}^{208}Pb_{gr} + {}^{208}Pb_{bl} + {}^{208}Pb_{tr}
\end{aligned} \tag{B.1}$$

where *gr* denotes a contribution from the Pb reference material used in the gravimetric U-Pb solution, *tr* from the tracer, and *bl* from the laboratory blank.

Assuming the signal at mass 201 is entirely $^{201}BaPO_2$, it can be used to subtract the isobaric interferences from underneath masses 202, 204, and 205. The ratios $^{202}BaPO_2/^{201}BaPO_2$, $^{204}BaPO_2/^{201}BaPO_2$, and $^{205}BaPO_2/^{201}BaPO_2$, calculated by considering all permutations of the constituent isotopes weighted by their relative abundance in nature (Böhlke et al., 2005), are calculated to be $1.4055 \times 10^{-3}$, $2.2259 \times 10^{-6}$, and $4.2206 \times 10^{-6}$, respectively. Expressing, for instance, the $^{202}BaPO_2$ contribution as the signal at mass 201 multiplied by the $^{202}BaPO_2/^{201}BaPO_2$, the $BaPO_2$ contributions may be subtracted from each measured mass.

The moles of each isotope of Pb can be normalized to $^{202}Pb$, which occurs only in the tracer. Likewise, the $BaPO_2$ can be normalized to the polyatomic ion with molecular weight 205.

$$\begin{aligned}
201_{tot}/{}^{202}Pb_{tr} &= {}^{201}BaPO_2/{}^{202}Pb_{tr} \\
202_{tot}/{}^{202}Pb_{tr} &= 1 + {}^{202}BaPO_2/{}^{202}Pb_{tr} \\
204_{tot}/{}^{202}Pb_{tr} &= {}^{204}Pb_{gr}/{}^{202}Pb_{tr} + {}^{204}Pb_{bl}/{}^{202}Pb_{tr} + {}^{204}Pb_{tr}/{}^{202}Pb_{tr} + {}^{204}BaPO_2/{}^{202}Pb_{tr} \\
205_{tot}/{}^{202}Pb_{tr} &= {}^{205}Pb_{tr}/{}^{202}Pb_{tr} + {}^{205}BaPO_2/{}^{202}Pb_{tr} \\
206_{tot}/{}^{202}Pb_{tr} &= {}^{206}Pb_{gr}/{}^{202}Pb_{tr} + {}^{206}Pb_{bl}/{}^{202}Pb_{tr} + {}^{206}Pb_{tr}/{}^{202}Pb_{tr} \\
207_{tot}/{}^{202}Pb_{tr} &= {}^{207}Pb_{gr}/{}^{202}Pb_{tr} + {}^{207}Pb_{bl}/{}^{202}Pb_{tr} + {}^{207}Pb_{tr}/{}^{202}Pb_{tr} \\
208_{tot}/{}^{202}Pb_{tr} &= {}^{208}Pb_{gr}/{}^{202}Pb_{tr} + {}^{208}Pb_{bl}/{}^{202}Pb_{tr} + {}^{208}Pb_{tr}/{}^{202}Pb_{tr}
\end{aligned} \tag{B.2}$$

The molar Pb ratios may now be recast in terms of the ratio of gravimetric solution and laboratory blank Pb to that in the tracer and the ICs of the three components. Likewise, the $BaPO_2$ contribution to each measured mass may be recast in terms of the ratio of $BaPO_2$ to tracer

and the $BaPO_2$ IC. This is accomplished by defining $r62gt$ and $r62bt$ as the ratio of the $^{206}$Pb contribution from the gravimetric solution and the laboratory blank to the $^{202}$Pb contribution from the tracer, respectively, and $r52BaPb$ as the ratio of the $^{205}BaPO_2$ to the $^{202}$Pb contribution from the tracer. The tracer IC is then expressed as the isotope ratios $r25t$, $r42t$, $r62t$, and $r72t$, representing $(^{202}\mathrm{Pb}/^{205}\mathrm{Pb})_{tr}$, $(^{204}\mathrm{Pb}/^{202}\mathrm{Pb})_{tr}$, and so on, and likewise for $r46b$, $r76b$, $r86b$ for the blank IC; $r46g$, $r76g$, $r86g$ for the gravimetric Pb reference material IC; and $r15Ba$, $r25Ba$, and $r45Ba$ for the ratios of $BaPO_2$ components. The measured signal at each mass can then be written as

$$
\begin{aligned}
201_{tot}/^{202}\mathrm{Pb}_{tr} &= r15Ba \cdot r52BaPb \\
202_{tot}/^{202}\mathrm{Pb}_{tr} &= 1 + r25Ba \cdot r52BaPb \\
204_{tot}/^{202}\mathrm{Pb}_{tr} &= r46g \cdot r62gt + r46b \cdot r62bt + r42t + r45Ba \cdot r52BaPb \\
205_{tot}/^{202}\mathrm{Pb}_{tr} &= 1/r25t + r52BaPb \\
206_{tot}/^{202}\mathrm{Pb}_{tr} &= r62gt + r62bt + r62t \\
207_{tot}/^{202}\mathrm{Pb}_{tr} &= r76g \cdot r62gt + r76b \cdot r62bt + r72t \\
208_{tot}/^{202}\mathrm{Pb}_{tr} &= r86g \cdot r62gt + r86b \cdot r62bt + r82t
\end{aligned}
\tag{B.3}
$$

Finally, the left hand side of equations (B.3) can be expressed as measured isotope ratios with $206_{tot}$ in the denominator by dividing each equation by the fifth equation in the system above, thereby reducing the number of equations to six. To equate the measured isotope ratios to the true IC of the sample, isotopic fractionation, or the preferential evaporation, ionization, and/or detection of light isotopes over heavier ones, must be considered as well. We use a modified exponential fractionation law (Russell et al., 1978), which has been shown empirically to closely model measured Pb isotopic data analyzed with a silica gel emitter (McLean, 2014).

Pb has also been observed to exhibit mass-independent fractionation (MIF), with odd-numbered isotopes preferentially evaporating and/or ionizing relative to the mass-dependent trend predicted by exponential fractionation (Doucelance and Manhès, 2001; Amelin et al., 2005; McLean, 2014). For large loads effectively free of isobaric interferences, this effect has been observed to remain constant throughout the analysis of a sample loaded on a single filament, and can be parameterized by a factor $\gamma$ that is unique to each isotope and is expected to be 1 for even-mass number isotopes. The modified exponential equation for two isotopes a and b thus takes the form (McLean, 2014)

$$
\left(\frac{a}{b}\right)_m = \left(\frac{a}{b}\right)_{true} \cdot \left(\frac{M_a \cdot \gamma_a}{M_b \cdot \gamma_b}\right)^{\beta} \tag{B.4}
$$

where $M_a$ and $M_b$ are the atomic masses of isotopes $a$ and $b$, and $(a/b)_m$ and $(a/b)_{true}$ are the measured and true (fractionation-corrected) isotope ratios, respectively. For clarity, the $\beta$ in equation (B.4) has the opposite sign but same absolute value as the conventional exponential fractionation equation.

Assuming $\gamma_{202} = \gamma_{204} = \gamma_{206} = \gamma_{208} = 1$ and adding the modified exponential fractionation term

to the resulting Pb isotope ratios produces the system of equations

$$
\begin{aligned}
r16m_j^i &= \frac{r15Ba \cdot r52BaPb_j^i}{r62t + r62gt^i + r62bt^i} \\
r26m_j^i &= \frac{1}{r62t + r62gt^i + r62bt^i}\left(\frac{M_{202}}{M_{206}}\right)^{\beta_j^i} + \frac{r25Ba \cdot r52BaPb_j^i}{r62t + r62gt^i + r62bt^i} \\
r46m_j^i &= \frac{r42t + r46g \cdot r62gt^i + r46b \cdot r62bt^i}{r62t + r62gt^i + r62bt^i}\left(\frac{M_{204}}{M_{206}}\right)^{\beta_j^i} + \frac{r45Ba \cdot r52BaPb_j^i}{r62t + r62gt^i + r62bt^i} \\
r56m_j^i &= \frac{1/r25t}{r62t + r62gt^i + r62bt^i}\left(\frac{M_{205} \cdot \gamma_{205}^i}{M_{206}}\right)^{\beta_j^i} + \frac{r52BaPb_j^i}{r62t + r62gt^i + r62bt^i} \\
r76m_j^i &= \frac{r72t + r76g \cdot r62gt^i + r76b \cdot r62bt^i}{r62t + r62gt^i + r62bt^i}\left(\frac{M_{207} \cdot \gamma_{207}^i}{M_{206}}\right)^{\beta_j^i} \\
r86m_j^i &= \frac{r82t + r86g \cdot r62gt^i + r86b \cdot r62bt^i}{r62t + r62gt^i + r62bt^i}\left(\frac{M_{208}}{M_{206}}\right)^{\beta_j^i}
\end{aligned}
\tag{B.5}
$$

where the superscripted index $i$ refers to an analysis and the subscripted index $j$ refers to an individual measured value. Thus each measurement must be corrected by a unique $r52BaPb$, or magnitude of $BaPO_2$ isobaric interference, and $\beta$, or magnitude of isotopic fractionation, which both change during the course of the analysis. Each analysis, which consists of multiple measurements, has a unique value for $r62gt$ and $r62bt$, which express the relative quantities of tracer, blank, and gravimetric solution, as well as $\gamma_{205}$ and $\gamma_{207}$, which quantify the degree of MIF for the odd-mass number Pb isotopes. Variables without indices, such as the tracer, Pb reference material, blank, and $BaPO_2$ ICs, are assumed to be constant for all analyses of the same gravimetric Pb reference material.

*Appendix B.2. Gravimetric-Tracer Mixture Pb Equations*

Unlike the data used in the Pb isotopic reference material inter-calibration in Section 2, the gravimetric-tracer Pb measurements, made at both NIGL and MIT, do not monitor the $BaPO_2$ isobaric interference. Because the Pb and U were loaded together and run on the same filament, Pb as $Pb^+$ at lower temperature, then U as $UO_2^+$ at higher temperature, the Pb was not run to the high temperatures at which $BaPO_2$ becomes a significant isobaric interference. Additionally, because the $^{204}Pb$ abundance is always less than an order of magnitude smaller than the other Pb isotopes, it does not contribute meaningfully to tracer calibration calculations, and has been ignored here. These omissions result in a simpler isotopic contribution budget than that used for the Pb

reference material inter-calibration,

$$
\begin{aligned}
202_{tot} &= {}^{202}\mathrm{Pb}_{tr} \\
205_{tot} &= {}^{205}\mathrm{Pb}_{tr} \\
206_{tot} &= {}^{206}\mathrm{Pb}_{gr} + {}^{206}\mathrm{Pb}_{bl} + {}^{206}\mathrm{Pb}_{tr} \\
207_{tot} &= {}^{207}\mathrm{Pb}_{gr} + {}^{207}\mathrm{Pb}_{bl} + {}^{207}\mathrm{Pb}_{tr} \\
208_{tot} &= {}^{208}\mathrm{Pb}_{gr} + {}^{208}\mathrm{Pb}_{bl} + {}^{208}\mathrm{Pb}_{tr}
\end{aligned}
\tag{B.6}
$$

where $tr$, $gr$, and $bl$ correspond to the tracer, gravimetric, and blank components, respectively, which sum to the total abundance of each isotope, denoted $tot$.

Normalizing equations (B.6) to $^{205}$Pb, which is present in both ET535 and ET2535 tracers but not in the gravimetric solutions, yields

$$
\begin{aligned}
\frac{202_{tot}}{{}^{205}\mathrm{Pb}_{tr}} &= \left(\frac{{}^{202}\mathrm{Pb}_{tr}}{{}^{205}\mathrm{Pb}_{tr}}\right) \\
\frac{206_{tot}}{{}^{205}\mathrm{Pb}_{tr}} &= \left(\frac{{}^{206}\mathrm{Pb}_{gr}}{{}^{205}\mathrm{Pb}_{tr}}\right) + \left(\frac{{}^{206}\mathrm{Pb}_{bl}}{{}^{205}\mathrm{Pb}_{tr}}\right) + \left(\frac{{}^{206}\mathrm{Pb}_{tr}}{{}^{205}\mathrm{Pb}_{tr}}\right) \\
\frac{207_{tot}}{{}^{205}\mathrm{Pb}_{tr}} &= \left(\frac{{}^{207}\mathrm{Pb}_{gr}}{{}^{205}\mathrm{Pb}_{tr}}\right) + \left(\frac{{}^{207}\mathrm{Pb}_{bl}}{{}^{205}\mathrm{Pb}_{tr}}\right) + \left(\frac{{}^{207}\mathrm{Pb}_{tr}}{{}^{205}\mathrm{Pb}_{tr}}\right) \\
\frac{208_{tot}}{{}^{205}\mathrm{Pb}_{tr}} &= \left(\frac{{}^{208}\mathrm{Pb}_{gr}}{{}^{205}\mathrm{Pb}_{tr}}\right) + \left(\frac{{}^{208}\mathrm{Pb}_{bl}}{{}^{205}\mathrm{Pb}_{tr}}\right) + \left(\frac{{}^{208}\mathrm{Pb}_{tr}}{{}^{205}\mathrm{Pb}_{tr}}\right)
\end{aligned}
\tag{B.7}
$$

The isotope ratios on the right hand side of equations (B.7) can be re-cast in terms of the isotope ratios of the gravimetric, tracer, and blank components. For instance, the ratio of $^{207}$Pb in the blank to $^{205}$Pb in the tracer can be expressed as the $^{207}$Pb/$^{206}$Pb of the blank, derived in Section 3, multiplied by the ratio of the moles of $^{206}$Pb in the blank to the moles of $^{205}$Pb in the tracer. Additionally, the isotope ratios on the left hand side of equations (B.7) can be expressed as measured isotope ratios when the 'true' isotope ratios on the right hand side are modified by fractionation correction factor (equation B.4). With these two substitutions, equations (B.7) become

$$
\begin{aligned}
\left(\frac{{}^{202}\mathrm{Pb}}{{}^{205}\mathrm{Pb}}\right)_m^{\frac{i}{j}} &= \left(\frac{{}^{202}\mathrm{Pb}}{{}^{205}\mathrm{Pb}}\right)_{tr} \left(\frac{M_{202}}{M_{205}\cdot\gamma_{205}^{i}}\right)^{\beta_j^i} \\
\left(\frac{{}^{206}\mathrm{Pb}}{{}^{205}\mathrm{Pb}}\right)_m^{\frac{i}{j}} &= \left[\left(\frac{{}^{206}\mathrm{Pb}_{gr}}{{}^{205}\mathrm{Pb}_{tr}}\right)^{i} + \left(\frac{{}^{206}\mathrm{Pb}_{bl}}{{}^{205}\mathrm{Pb}_{tr}}\right)^{i} + \left(\frac{{}^{206}\mathrm{Pb}}{{}^{205}\mathrm{Pb}}\right)_{tr}\right] \left(\frac{M_{206}}{M_{205}\cdot\gamma_{205}^{i}}\right)^{\beta_j^i} \\
\left(\frac{{}^{207}\mathrm{Pb}}{{}^{205}\mathrm{Pb}}\right)_m^{\frac{i}{j}} &= \left[\left(\frac{{}^{207}\mathrm{Pb}}{{}^{206}\mathrm{Pb}}\right)_{gr} \left(\frac{{}^{206}\mathrm{Pb}_{gr}}{{}^{205}\mathrm{Pb}_{tr}}\right)^{i} + \left(\frac{{}^{207}\mathrm{Pb}}{{}^{206}\mathrm{Pb}}\right)_{bl} \left(\frac{{}^{206}\mathrm{Pb}_{bl}}{{}^{205}\mathrm{Pb}_{tr}}\right)^{i} + \left(\frac{{}^{207}\mathrm{Pb}}{{}^{205}\mathrm{Pb}}\right)_{tr}\right] \left(\frac{M_{207}\cdot\gamma_{207}^{i}}{M_{205}\cdot\gamma_{205}^{i}}\right)^{\beta_j^i} \\
\left(\frac{{}^{208}\mathrm{Pb}}{{}^{205}\mathrm{Pb}}\right)_m^{\frac{i}{j}} &= \left[\left(\frac{{}^{208}\mathrm{Pb}}{{}^{206}\mathrm{Pb}}\right)_{gr} \left(\frac{{}^{206}\mathrm{Pb}_{gr}}{{}^{205}\mathrm{Pb}_{tr}}\right)^{i} + \left(\frac{{}^{208}\mathrm{Pb}}{{}^{206}\mathrm{Pb}}\right)_{bl} \left(\frac{{}^{206}\mathrm{Pb}_{bl}}{{}^{205}\mathrm{Pb}_{tr}}\right)^{i} + \left(\frac{{}^{208}\mathrm{Pb}}{{}^{205}\mathrm{Pb}}\right)_{tr}\right] \left(\frac{M_{208}}{M_{205}\cdot\gamma_{205}^{i}}\right)^{\beta_j^i}
\end{aligned}
\tag{B.8}
$$

where $i$ denotes a variable that changes from load to load and $j$ denotes a variable that additionally changes from block to block. In this system, the variables corresponding to the blank, tracer,

and gravimetric solution Pb ICs are all treated as known variables, with maximum likelihood estimates and uncertainties reported above. The ratio of the blank to the tracer, embodied in the $^{206}Pb_{bl}/^{205}Pb_{tr}$ can be estimated from tracer mass used and total procedural blank measurements. Following McLean (2014) the mass-independent fractionation parameterized with the $\gamma$ terms is assumed to remain constant for each load but vary between loads, and the absolute magnitude of fractionation, $\beta$ changes during the course of each analysis. For gravimetric solution mixtures with ET535, the first equation that includes $^{202}Pb$ is ignored.

For the corresponding U measurement, the same system used for the critical mixtures in equations (B.13) applies. Because the magnitude of isotopic fractionation changes dramatically during the long gravimetric-tracer mixture analyses, the parameter $\beta$ is allowed to change from block to block. The paired Pb and U measurements combine to form a large overdetermined system of equations, with each block of data contributing five or six measured ratios, depending on whether $^{202}Pb$ is present. Using the gravimetric solution $^{206}Pb/^{238}U$ calculated from equations (7) and (8), and the $(^{238}U_{gr}/^{235}U_{tr})$ from equations (B.13), the term $(^{206}Pb_{gr}/^{205}Pb_{tr})$ can be recast as

$$\left(\frac{^{206}\mathrm{Pb}_{gr}}{^{205}\mathrm{Pb}_{tr}}\right)^{i} = \left(\frac{^{235}\mathrm{U}}{^{205}\mathrm{Pb}}\right)_{tr} \cdot \left(\frac{^{206}\mathrm{Pb}}{^{238}\mathrm{U}}\right)_{gr} \cdot \left(\frac{^{238}\mathrm{U}_{gr}}{^{235}\mathrm{U}_{tr}}\right)^{i} \tag{B.9}$$

Substituting the right-hand side expression (B.9) into equations (B.8), along with equations (B.13) for U measurements, creates a system of five equations for ET535 measurements, or six equations for ET2535 measurements that relate measured Pb and U isotope ratios to the gravimetric and tracer solution ICs and their U/Pb ratios.

*Appendix B.3. U Model*

The isotopic composition of all critical mixtures and tracer ICs were measured as $UO_2$ (Condon et al., in review). Isobaric interference corrections were made on each cycle, and the mean and standard error of the resulting U ratios represent the best estimate of the fractionated IC of the sample. Expressing the components that make up a mixture of the ET(2)535 tracer with a reference material, such as SRM U500 or CRM 112a,

$$\begin{aligned} 233_{tot} &= 233_{tr} \\ 235_{tot} &= 235_{st} + 235_{bl} + 235_{tr} \\ 238_{tot} &= 238_{st} + 238_{bl} + 238_{tr} \end{aligned} \tag{B.10}$$

where *st* denotes the contribution from an isotopic reference material, *tr* from the tracer, and *bl* from the blank.

Normalizing all the components to the moles of $^{235}U$ in the tracer results in

$$\begin{aligned} 233_{tot}/235_{tr} &= (233_{tr}/235_{tr}) \\ 235_{tot}/235_{tr} &= (235_{st}/235_{tr}) + (235_{bl}/235_{tr}) + (235_{tr}/235_{tr}) \\ 238_{tot}/235_{tr} &= (238_{st}/235_{tr}) + (238_{bl}/235_{tr}) + (238_{tr}/235_{tr}) \end{aligned} \tag{B.11}$$

Recasting the mixed component ratios ($235_{bl}/235_{tr}$) as ($238_{bl}/235_{tr}$) / ($238_{bl}/235_{bl}$) and ($235_{st}/235_{tr}$) as ($238_{st}/235_{tr}$) / ($238_{st}/235_{st}$) yields

$$\begin{aligned} 233_{tot}/235_{tr} &= r35t \\ 235_{tot}/235_{tr} &= r85st/r85s + r85bt/r85b + 1 \\ 238_{tot}/235_{tr} &= r85st + r85bt + r85t \end{aligned} \tag{B.12}$$

where $r35t$ and $r85t$ are the tracer parameters that are being determined, $r85b$ and $r85s$ are the $^{238}U/^{235}U$ of the blank and the isotopic reference material, respectively, and $r85st$ and $r85bt$ are the moles of $^{238}U$ in the reference material and blank, respectively, relative to the moles of $^{235}U$ in the tracer.

Dividing the first and third equations by the second equation yields the U ratios as commonly measured. In order to equate the true and measured ratios, an exponential fractionation term is added as well.

$$\begin{aligned} r35m^i &= \frac{r35t}{1 + r85bt^i/r85b + r85st^i/r85s}\left(\frac{M_{233}}{M_{235}}\right)^{\beta^i} \\ r85m^i &= \frac{r85bt^i + r85st^i + r85t}{1 + r85bt^i/r85b + r85st^i/r85s}\left(\frac{M_{238}}{M_{235}}\right)^{\beta^i} \end{aligned} \tag{B.13}$$

where $M_x$ denotes the isotopic mass of $x$ and the superscript $i$ denotes variables that change from one analysis to the next. These two equations apply to each measurement of a critical mixture made, regardless of the isotopic reference material used. For measurements of the tracer only, which also include a loading blank, the $r85s$ and $r85st$ terms may be dropped.

## Bibliography


Amelin Y., Davis D.W. and Davis W.J. (2005) Decoupled fractionation of even- and odd-mass isotopes of Pb in TIMS. *Geochimica et Cosmochimica Acta* **69**(10), A215.

Amelin Y. and Davis W.J. (2006) Isotopic analysis of lead in sub-nanogram quantities by TIMS using a $^{202}$Pb-$^{205}$Pb spike. *Journal of Analytical Atomic Spectrometry* **21**(10), 1053–1061.

Audi G., Wapstra A.H. and Thibault C. (2003) The Ame2003 atomic mass evaluation: (II). Tables, graphs and references. *Nuclear Physics A* **729**(1), 337–676.

Baker J., Peate D., Waight T. and Meyzen C. (2004) Pb isotopic analysis of standards and samples using a $^{207}$Pb-$^{204}$Pb double spike and thallium to correct for mass bias with a double-focusing MC-ICP-MS. *Chemical Geology* **211**(3-4), 275–303.

Böhlke J.K., de Laeter J.R., Bièvre P.D., Hidaka H., Peiser H.S., Rosman K.J.R. and Taylor P.D.P. (2005) Isotopic compositions of the elements, 2001. *Journal of Physical and Chemical Reference Data* **34**(1), 57–67.

Catanzaro E.J., Murphy T.J., Shields W.R. and Garner E.L. (1968) Absolute isotopic abundance ratios of common, equal-atom, and radiogenic lead standards. *Journal of Research of the National Bureau of Standards - A. Physics and Chemistry* **72A**(3), 261–267.

836 Cheng H., Lawrence Edwards R., Shen C.C., Polyak V.J., Asmerom Y., Woodhead J., Hellstrom
837 J., Wang Y., Kong X., Spötl C., Wang X. and Calvin Alexander Jr. E. (2013) Improvements in
838 $^{230}$Th dating, $^{230}$Th and $^{234}$U half-life values, and U–Th isotopic measurements by multi-collector
839 inductively coupled plasma mass spectrometry. *Earth and Planetary Science Letters* **371–372**(0),
840 82–91.

841 Condon D.J., McLean N., Noble S.R. and Bowring S.A. (2010) Isotopic composition ($^{238}$U/$^{235}$U)
842 of some commonly used uranium reference materials. *Geochimica et Cosmochimica Acta* **74**,
843 7127–7143.

844 Condon D.J., Schoene R.B., McLean N.M., Parrish R. and Bowring S.A. (in review) Metrology and
845 traceability of U-Pb isotope dilution geochronology (EARTHTIME tracer calibration Part I),
846 submitted to Geochem. Geophys. Geosyst.

847 Corfu F. and Dahlgren S. (2008) Perovskite U–Pb ages and the Pb isotopic composition of alkaline
848 volcanism initiating the Permo-Carboniferous Oslo Rift. *Earth and Planetary Science Letters*
849 **265**(1–2), 256–269.

850 Doucelance R. and Manhès G. (2001) Reevaluation of precise lead isotope measurements by
851 thermal ionization mass spectrometry: comparison with determinations by plasma source mass
852 spectrometry. *Chemical Geology* **176**(1-4), 361–377.

853 Galer S.J.G. (1999) Optimal double and triple spiking for high precision lead isotopic measurement.
854 *Chemical Geology* **157**(3–4), 255–274.

855 Hiess J., Condon D.J., McLean N. and Noble S.R. (2012) $^{238}$U/$^{235}$U systematics in terrestrial
856 U-bearing minerals. *Science* **335**(6076), 1610–1614.

857 Hofmann A. (1971) Fractionation corrections for mixed-isotope spikes of Sr, K, and Pb. *Earth and*
858 *Planetary Science Letters* **10**(4), 397–402.

859 Jaffey A.H., Flynn K.F., Glendenin L.E., Bentley W.C. and Essling A.M. (1971) Precision measure-
860 ment of half-lives and specific activities of $^{235}$U and $^{238}$U. *Phys. Rev.* **C**(4), 1889–1906.

861 Krogh T.E. (1964) Strontium isotopic variation and whole rock isochron studies in the Grenville
862 Province of Ontario. *MIT Annual Progress Reports (AEC Contract AT(30-1)-1381)* **12**, 73.

863 Mattinson J.M. (2010) Analysis of the relative decay constants of $^{235}$U and $^{238}$U by multi-step
864 CA-TIMS measurements of closed-system natural zircon samples. *Chemical Geology* **275**(3-4),
865 186–198.

866 McLean N.M. (2014) Straight line regression through data with correlated uncertainties in two or
867 more dimensions, with an application to kinetic isotope fractionation. *Geochimica et Cosmochimica*
868 *Acta* **124**(0), 237–249.

869 McLean N.M., Bowring J.F. and Bowring S.A. (2011) An algorithm for U-Pb isotope dilution data
870 reduction and uncertainty propagation. *Geochem. Geophys. Geosyst.* **12**.

871 Nebel O., Scherer E.E. and Mezger K. (2011) Evaluation of the $^{87}$Rb decay constant by age
872 comparison against the U–Pb system. *Earth and Planetary Science Letters* **301**(1–2), 1–8.

Renne P.R., Mundil R., Balco G., Min K. and Ludwig K.R. (2010) Joint determination of $^{40}$K decay constants and $^{40}$Ar$^*$/$^{40}$K for the Fish Canyon sanidine standard, and improved accuracy for $^{40}$Ar/$^{39}$Ar geochronology. *Geochimica et Cosmochimica Acta* **74**(18), 5349–5367.

Rioux M., Johan Lissenberg C., McLean N.M., Bowring S.A., MacLeod C.J., Hellebrand E. and Shimizu N. (2012) Protracted timescales of lower crustal growth at the fast-spreading East Pacific Rise. *Nature Geoscience* **5**(4), 275–278.

Rotenberg E., Davis D.W., Amelin Y., Ghosh S. and Bergquist B.A. (2012) Determination of the decay-constant of 87rb by laboratory accumulation of 87sr. *Geochimica et Cosmochimica Acta* **85**(0), 41–57.

Rudge J.F., Reynolds B.C. and Bourdon B. (2009) The double spike toolbox. *Chemical Geology* **265**(3–4), 420–431.

Russell W.A., Papanastassiou D.A. and Tombrello T.A. (1978) Ca isotope fractionation on the Earth and other solar system materials. *Geochimica et Cosmochimica Acta* **42**(8), 1075–1090.

Schmitz M.D. and Schoene B. (2007) Derivation of isotope ratios, errors, and error correlations for U-Pb geochronology using $^{205}$Pb-$^{235}$U-($^{233}$U)-spiked isotope dilution thermal ionization mass spectrometric data. *Geochem. Geophys. Geosyst.* **8**(8).

Schoene B., Crowley J.L., Condon D.J., Schmitz M.D. and Bowring S.A. (2006) Reassessing the uranium decay constants for geochronology using ID-TIMS U–Pb data. *Geochimica et Cosmochimica Acta* **70**(2), 426–445.

Stirling C.H., Andersen M.B., Potter E.K. and Halliday A.N. (2007) Low-temperature isotopic fractionation of uranium. *Earth and Planetary Science Letters* **264**(1–2), 208–225.

Stracke A., Scherer E. and Reynolds B. (2014) 15.4 - application of isotope dilution in geochemistry. In *Treatise on Geochemistry (Second Edition)* (eds. H.D. Holland and K.K. Turekian), pp. 71–86, Elsevier, Oxford.
**URL:** *http://www.sciencedirect.com/science/article/pii/B9780080959757014042*

Tarantola A. (2005) *Inverse Problem Theory and Methods for Model Parameter Estimation*. SIAM, Philadelphia, Pennsylvania.

Tarantola A. and Valette B. (1982a) Generalized nonlinear inverse problems solved using the least squares criterion. *Review of Geophysics and Space Physics* **20**, 219–232.

Tarantola A. and Valette B. (1982b) Inverse problems = quest for information. *Journal of Geophysics* **50**, 159–170.

Tilton G.R., Patterson C., Brown H., Inghram M., Hayden R., Hess D. and Larsen E. (1955) Isotopic composition and distribution of lead, uranium, and thorium in a Precambrian granite. *Geological Society of America Bulletin* **66**(9), 1131–1148.

Todt W., Cliff R., Hanser A. and Hofmann A. (1996) *Evaluation of a $^{202}$Pb-$^{205}$Pb Double Spike for High-Precision Lead Isotope Analysis*, vol. 95, Earth Processes: Reading the Isotopic Code of *Geophysical Monographs*, pp. 429–437. American Geophysical Union.

Verbruggen A., Eykens R., Kehoe F., Kühn H., Richter S. and Aregbe Y. (2008) *Preparation and Certification of IRMM-3636, IRMM-3636a and IRMM-3636b*. Tech. rep., JRC Scientific and Technical Reports.
**URL:** *http://publications.jrc.ec.europa.eu/repository/handle/111111111/4450*

Vermeesch P. (2010) Helioplot, and the treatment of overdispersed (U-Th-Sm)/He data. *Chemical Geology* **271**(3-4), 108–111.

Vervoort J.D., Patchett P.J., Sderlund U. and Baker M. (2004) Isotopic composition of yb and the determination of lu concentrations and lu/hf ratios by isotope dilution using mc-icpms. *Geochem. Geophys. Geosyst.* **5**(11), Q11002–.

Wasserburg G., Jacousen S., DePaolo D., McCulloch M. and Wen T. (1981) Precise determination of Sm/Nd ratios, Sm and Nd isotopic abundances in standard solutions. *Geochimica et Cosmochimica Acta* **45**(12), 2311–2323.

Wetherill G.W. (1956) Discordant uranium-lead ages, I. *Transactions, American Geophysical Union* **37**, 320–326.

Weyer S., Anbar A.D., Gerdes A., Gordon G.W., Algeo T.J. and Boyle E.A. (2008) Natural fractionation of $^{238}U/^{235}U$. *Geochimica et Cosmochimica Acta* **72**(2), 345–359.